The Thesis committee for David Aaron Christiansen

Certifies that this is the approved version of the following thesis:

Flow Around a Dredge Spoil Island in a Shallow Estuary During Peak Tidal Currents

APPROVED BY
SUPERVISING COMMITTEE:

Supervisor:____

Ben R. Hodges

____

Paola Passalacqua

Flow Around a Dredge Spoil Island in a Shallow Estuary During Peak Tidal Currents

by

David Aaron Christiansen, B.S.

Thesis

Presented to the Faculty of the Graduate School
of the University of Texas at Austin
in Partial Fulfillment
of the Requirements
for the Degree of

Master of Science in Engineering

The University of Texas at Austin
December, 2013

Acknowledgements

I would like to take this opportunity to thank the many people and organizations that have helped me reach my goal. First, I'd like to thank my advisor, Dr. Ben Hodges for all of his guidance and patience throughout my time here at UT Austin. I'd like to thank Abigail Tomasek, Garrett Kehoe, and Matthew Rayson for their invaluable help during data collection trips. They made my field experience a much more enjoyable one, and probably prevented many nervous breakdowns along the way. I'd also like to thank all of the faculty, especially Dr. Paola Passalacqua for being on my committee, and students in EWRE for making my experience as a Longhorn a memorable and enjoyable one. I'd like to thank my family and friends for supporting me, both emotionally and financially, as I strived to accomplish my master's work. Finally, I'd like to thank the City of Houston for being a beacon during dark nights on the water. Without those lights we might have been lost on many occasions.

This research was funded as part of the Gulf Integrated Spill Response (GISR) consortium by the Gulf of Mexico Research Initiative (GoMRI). I thank them for their contribution, and for the work they are doing to advance the field of oil spill research.

Flow Around a Dredge Spoil Island in a Shallow Estuary During Peak Tidal Currents

by

David Aaron Christiansen, MSE

The University of Texas at Austin, 2013

SUPERVISOR: Ben R. Hodges

A vessel-mounted ADCP study focusing on channel-scale flow patterns in Galveston Bay near the Houston Shipping Channel and Mid-Bay Island is described. Winds of 5-7 m/s at 215-230° from N were present during data collection. For both peak ebb and flood conditions, the tidal circulation forced flow in a direction opposing the wind, perhaps due to a large-scale flow divergence forced by Mid-Bay Island. The strongest such currents were measured closest the island.

During peak flood flow, the shape of the along-channel velocity profile for the open water upwind of the channel at Mid-Bay Island indicated uniform flow, and the salinity profile indicated a well-mixed water column. The near-island along-channel velocity profile showed a near-linear trend, and the salinity profile indicated a stratified water column. This suggested that the stratification had some effect the velocity profile shape, but further research is needed to better quantify this effect.

During peak ebb flow, the near-island along-channel velocities were highly variable with respect to the mean velocity, indicating an area of active turbulence. Salin-

ity profiles collected in the open water and near-island both showed stratification, something that was not seen during flood conditions.

Differences in observations between flood and ebb flows can possibly be attributed to the survey location with respect to the chain of dredge spoil islands. During flood flows Mid-Bay Island is the first of the islands, and the flows surrounding the island may part of a developing horizontal boundary layer. During ebb flows the island is last in the chain relative to the direction of flow, and therefore the surrounding flows are well back from the leading edge of a horizontal boundary layer.

Table of Contents

List of Figures

List of Tables

Chapter 1 - Introduction

The field study discussed in this report was funded by the Gulf of Mexico Research Initiative (GoMRI) as part of the Gulf Integrated Spill Response (GISR) consortium. GoMRI was created after the Deep Water Horizon catastrophe in the Gulf of Mexico in 2010. This disaster released approximately 5 million barrels of oil and 100 million ft^3 of natural gas into the environment, and killed 11 workers (WHOI, 2011). GoMRI was funded in large part by the damages paid by BP as a result of its lawsuit, and aims to improve predictive capabilities related to oil-spill modeling, to improve methods of oil-spill clean up, and to further study the effects felt by the manmade and natural environments in the wake of such a spill (GoMRI, 2013). As a part of GoMRI, the GISR consortium focuses on studying and predicting the interactions of petroleum with open ocean water (Chapman, 2013).

Within the GISR project, this study focused on collecting data to support the development of a bay-scale hydrodynamic model whose current predictions can be used with oil spill trajectory models. Velocity and salinity data were obtained using an acoustic Doppler current profiler (ADCP) and a conductivity-temperature-depth (CTD) sensor in Galveston Bay, located along the Texas Gulf Coast near Houston, TX. This data was processed and provided to the GISR team using the Stanford Unstructured Nonhydrostatic Terrain-following Adaptive Navier-Stokes Simulator (SUNTANS) model (Fringer et al., 2006).

The data were collected along three transects crossing the Houston Shipping Channel at several locations within Galveston Bay, shown in Fig. 1. The northernmost transect (herein Transect 1), included the water in the channel between navigational channel markers 67 and 68, as well as the shallower regions to the immediate southwest of those markers and between the shipping channel and the dredge spoil island known as Mid-Bay Island. Transect 2 included the water in the channel between markers 45 and 46 and the shallower regions on either side of the channel. Transect 3, near the mouth of Galveston Bay, passed from the southeastern point of the Texas City Dike to the southwestern point of the barrier island to the northwest of the intracoastal waterway. Data were collected along each of these transects every two weeks from June 2013 to early August 2013, coinciding with peak spring ebb and peak spring flood tidal currents. This report focuses on analysis of Transect 1 data collected near Mid-Bay Island during the field study from August 5 – 7, 2013. Metadata associated with all the field studies are provided in A and B. Full data are available through the GoMRI website at `data.gulfresearchinitiative.org`.

Figure 1: Transect locations for data collection in Galveston Bay. Mid-Bay Island cannot be seen due to the age of the image. (Image source: ArcGIS from ESRI, i-cubed, USDA, USGS, AEX, GeoEye, Getmapping, Aerogrid, IGN, IGP, and the GIS User Community)

Chapter 2 - Background

2.1 Overview

Water velocity profiles have been previously collected in coastal and bay systems (including Galveston Bay) using ADCP instruments. These devices have been deployed in a downward-looking mode from shipboard and buoys, and in an upward-looking mode mounted on the bay bottom. In Galveston Bay, ADCP studies have focused on flows in the Houston Ship Channel. The flows in Galveston Bay are affected by wind, river inflows, and tidal exchange with the Gulf of Mexico. Outside of significant storm events, the river inflows are a small relative to the tidal fluxes at the Bay mouth. Because the Bay is shallow and broad, consistent winds affect the circulation, although the depth of the ship channel ($\sim 4\times$ Bay depth) limits the ability of the wind to affect deep in-channel flows. The present study is focused on flows in and near the ship channel in the vicinity of Mid-Bay Island, which did not exist when the last major ADCP survey was conducted by Schmalz (2000).

2.2 ADCP Use in Shallow Estuaries

The first ADCP was developed for use in deep sea applications in 1975 by researchers at Scripps Institute of Oceanography (Pinkel, 1979). These instruments have been utilized in collecting many kinds of data in a variety of settings ranging from microorganism population estimation in the Antarctic (e.g. Zhou et al., 1994; Brierley et al., 1998; Espinasse et al., 2012), to flux calculation in rivers (e.g. Callede et al., 2000; Dinehart and Burau, 2005; Filizola and Guyot, 2004; Szupiany et al., 2007), to hydrodynamic studies in shallow estuaries. Herein, the focus is on the latter case.

In shallow estuary hydrodynamic surveys, the ADCP mounting affects the scope of the data collected. For example, ADCPs in bottom-mounted configurations (*i.e.* an upward-looking profiler that is anchored to the bottom) are used to collect velocity profiles over time at a single geographic location (e.g. Lerczak et al., 2009; Ralston et al., 2008). Conversely, vessel-mounted configurations (*i.e.* where the unit is attached directly to or towed by the research vessel) provide data over a larger space, but over a limited time interval (e.g. Barth and Brink, 1987; Marmorino and Trump, 1996; Scully and Geyer, 2012). Surveys can range from hours (e.g. O'Donnell et al., 1998) to months or even years of data collection (e.g. Buijsman and Ridderinkhof, 2007; Reed et al., 2004), depending on the scales of interest.

ADCPs are often used in conjunction with other equipment to more completely describe flow conditions. For example, Geyer et al. (2000) used a ship-mounted ADCP, CTD, ship-mounted current meters, as well as a bottom-mounted ADCP to describe the flow in the Hudson River estuary. In Corpus Christi Bay, TX, Ojo et al. (2006) used a ship-mounted ADCP to calculate turbulent diffusivity values, which were then calibrated using the results of a simultaneous dye tracer study.

ADCP surveys can be designed for multiple objectives: model calibration/validation (e.g. Ralston et al., 2008), estimation of turbulence (e.g. MacDonald and Geyer, 2004; Trowbridge et al., 1999), and characterization of larger scale flow patterns (e.g. Chant and Wilson, 1997; Marmorino and Trump, 1996; Old and Vennell, 2001). In many cases, ADCP data can serve multiple purposes (*e.g.* both model calibration and characterization of larger scale flow patterns).

The present work uses a downward-looking, vessel-mounted ADCP and a CTD to quantify flow patterns in a relatively small portion of Galveston Bay.

2.3 Study Site: Galveston Bay

Galveston Bay is located along the Texas Gulf Coast to the southeast of Houston, TX. The Bay is a shallow estuary, receiving fresh water inflow from the San Jacinto and Trinity Rivers and saltwater from the Gulf of Mexico through dredged channels in barrier islands. Excluding the Houston Shipping Channel, the Bay has a mean depth of 1.64 m at mean low water with a standard deviation of 0.87 m (Department of Commerce (DOC); National Oceanic and Atmospheric Administration (NOAA), 1998). The channel runs from the mouth of Galveston Bay near Port Bolivar north by northeast through the San Jacinto River delta into Houston. The channel has existed in some form since 1876 (Sibley, 2013), and today is dredged to an authorized depth of 45 ft with a overdepth of 2 ft (Casebeer, 2013) . Channel sediment extracted during episodic dredging (every 1-7 years depending on funding and location) has been deposited in 13 dredged material areas, several of which are dredge spoil islands running along the eastern side of the northern channel (Casebeer, 2013). The flow regime around Mid Bay Island (Transect 1 in Fig. 1), located at 29° 34' 37.30" N 94° 55' 03.44" W, is the focus of this study.

2.4 Flows in Galveston Bay

Galveston Bay receives approximately 11 km^3/year, or 348 m^3/s, of freshwater from sources listed in Table 1. To put the freshwater inflows into perspective, the mean velocity ($v = QA^{-1}$) at the Bay mouth associated with the river flows can be compared to the tidal currents. The cross-sectional area at the mouth is $A \approx$77,000 m^2, so the mean river velocity contribution is 2.5×10^{-3} m/s. The peak tidal currents, which routinely occur, are O(1m/s), which dwarfs the river velocity. However, significant storm events can occasionally provide river fluxes that are on the scale of 1/5 of the tidal fluxes (USGS, 2013).

Table 1 Sources of freshwater inflow to Galveston Bay (Wermund, 1989)

Source	Freshwater Inflow (km^3/yr)
San Jacinto River	1.73
Trinity River	6.17
Local Runoff	3.08

Fig. 2 shows the locations within the Bay where different kinds of data are available from other sources. The red and yellow markers indicate buoys that report tidal elevation, meteorological observations, and water temperature and conductivity. The cyan markers indicate buoys that are supposed to report velocity data. However, the only velocity data presently available is provided by a downward-looking ADCP attached to the buoy labeled Galveston Bay Entr Channel LB 11 (NOAA, 2013b).

In 1999, NOAA and Texas A&M University worked in partnership to conduct a field study of the Houston Shipping Channel (Schmalz, 2000). The objective was to quantify fluxes and flow patterns from water velocity data collected using a towed ADCP along 5 transects crossing a region of the channel to the northeast of Eagle Point, as shown in Fig. 3.

The Schmalz study was conducted before spoils began to be dumped at what is

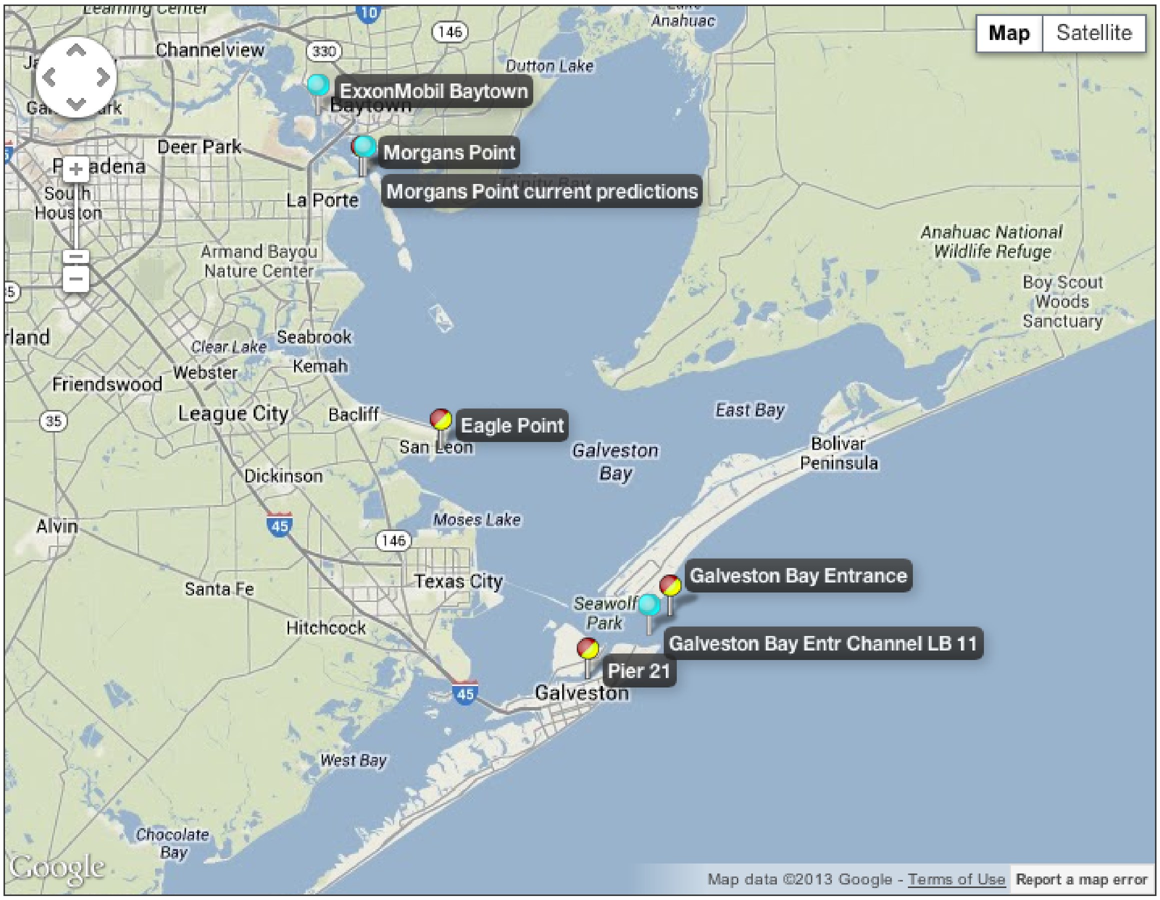

Figure 2: Map of Galveston Bay with locations of NOAA National Data Buoy Center (NDBC) buoys. Red and yellow markers indicate meteorological and tidal data buoys, and cyan markers indicate water velocity data buoys (NOAA, 2013b).

Figure 3: Map of transect locations from Schmalz, 2000. (Image source: ArcGIS from ESRI, i-cubed, USDA, USGS, AEX, GeoEye, Getmapping, Aerogrid, IGN, IGP, and the GIS User Community)

now Mid Bay Island (Griffin, 2009). This island is hypothesized to have significantly affected the flow both in the channel, due to its close proximity, and in the nearby shallow regions. The transect label T5 in Schmalz (2000) is identical Transect 1 discussed in the present work. Unfortunately, analyses of T5 data are not provided in Schmalz (2000), so comparisons with the present study could not be made.

Other studies involving flows in Galveston Bay have focused on oyster population change (see Klinck et al., 2002) and sediment/nutrient transport (e.g. Phillips et al., 2004; Sahl et al., 1993; Warnken et al., 2000; Yeager et al., 2007). These studies used bay-scale flow circulation models of Galveston Bay. Because of the relatively small footprint of Mid-Bay Island in comparison to the overall Bay footprint, the effects of the island on flow patterns in the area were inadvertently excluded in these studies.

The flow effects of Mid-Bay Island have not been previously studied, either due to its relatively small footprint, causing it to be ignored in bay-scale models, or because of its relatively recent date of creation. Thus, the goal of this research is to characterize any effects caused by the island on the flows both in the Houston Shipping Channel and in the shallower areas to either side of the channel, as well as posit some future research ideas to further quantify these effects.

Chapter 3 - Methods

3.1 Overview

A downward-looking ADCP was deployed from a 23 ft boat along a transect perpendicular to Mid Bay Island and the Houston Shipping Channel. Salinity profiles during the study were obtained with at CTD profiler. Tidal conditions during the transect data collection were near maximum ebb and flood. Transect data are analyzed averaging over zones, which are defined as the deep channel and the shallow bay on either side of the channel.

3.2 Instrumentation

Water velocity data were collected with a Sontek/YSI M9 ADCP using Sontek/YSI RiverSurveyor software. The ADCP unit has 9 transducers, which operate at three frequencies. Fig. 4 shows the configuration and operating frequency of each set of transducers, as well as the location of the temperature sensor. The 0.5 MHz transducer is used for depth measurement and bottom tracking. The combination of 1 and 3 MHz transducers allows the unit to measure water velocities at a higher resolution and greater depth range when compared to other, single frequency models (Sontek/YSI, 2012b). The M9 ADCP can measure depths from 0.20 to 80 m, and can measure water velocities from 0.06 to 40 m depth. It has a resolution of 0.1 cm/s, and can divide the water column being surveyed into as many as 128 bins at a bin size of 0.02 to 4 m (Sontek/YSI, 2012b). The complete system consisting of the M9 ADCP transducer unit, a power and communications module (PCM), and a differential global positioning system (DGPS) are all manufactured by Sontek.

When assembling the system for data collection, the ADCP connected to the PCM with a waterproof 8-pin cable. The DGPS also connected to the PCM using a simple coaxial cable. The PCM communicated both the ADCP and DGPS data streams via Bluetooth to a mobile device equipped with RiverSurveyor software. All data was recorded on the ADCP during the field study, and downloaded to a laptop computer running the Windows operating system for analyses. The settings used during data collection are outlined in Table 2.

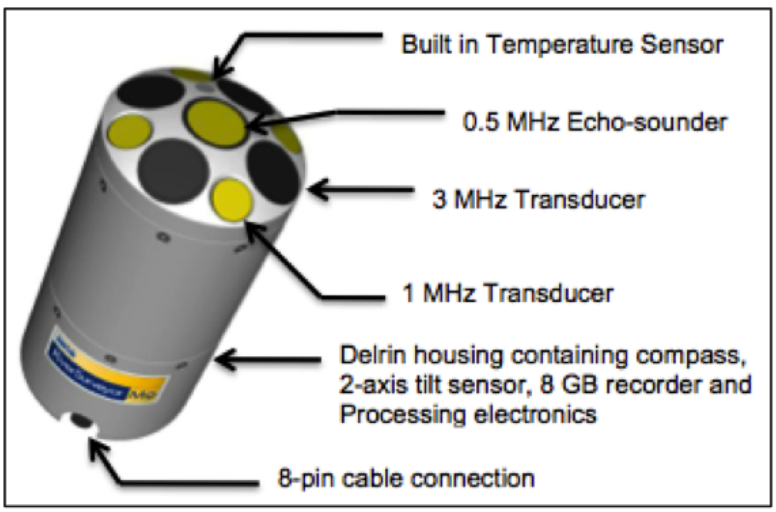

Figure 4: Sontek M9 ADCP features (Sontek/YSI, 2012b)

Fig. 5 shows a sketch of the location of the ADCP and DGPS units on the boat. The ADCP unit was mounted off the starboard side of a 23-foot, flat-bottom boat using a mounting arm constructed from schedule 80, 2-inch-diameter PVC and aluminum L-angle structural beams (Fig. 6).

To provide a valid measurement, the ADCP transducer head must be submerged. A transducer depth of 0.15 m in still water was sufficient to keep the transducers

Table 2 RiverSurveyor System Settings

Transducer Depth (m)	0.15
Screening Distance (m)	0.0
Salinity (ppt)	29.0 (retroactively corrected using CTD data)
Magnetic Declination (deg)	0.0
SonTek Compass Heading Corr (deg)	0.0
GPS Antenna X Offset (m)	0.5
GPS Antenna Y Offset (m)	0.2
Track Reference	Bottom-Track
Depth Reference	Vertical Beam
Coordinate System	ENU
SmartPulseHD	Enabled
Left Edge Distance (m)	0.0
Left Edge Method	Vertical Bank
Right Edge Distance (m)	0.0
Right Edge Method	Vertical Bank

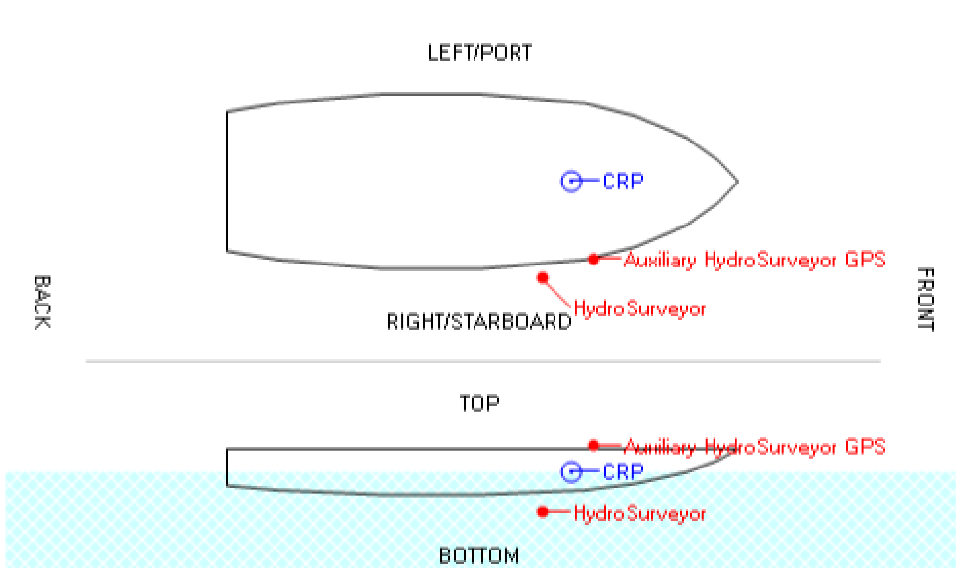

Figure 5: Layout of Instrumentation within the boat

Figure 6: Mounting arm for boat-mounted ADCP configuration

under water at all times while underway. Typical waves/swell height during the survey were visually estimated at 0.5 m; however, because the boat was small enough to move with the swell, the ADCP transducers remained submerged. Data were collected at 4-5 knots to prevent cavitation at the transducer head and vibrations in the mounting arm, which are known to introduce data errors (Velasco, 2012). The ADCP has a blanking distance of 0.5 m, meaning that anything closer to the transducer head than 0.5 m cannot be measured. This blanking distance plus the transducer depth meant that the top 0.65 m of the water column was not be measured during data collection.

A YSI CastAway conductivity, temperature, and depth sensor (CTD) was used to correct the sound speed of the ADCP measurements and to collect salinity, temperature, and density profiles. The capabilities of this unit are provided in Table 3. The CTD was deployed from the end of a fishing rod equipped with 65 lb. test line. The unit was allowed to fall at a rate of 1 m/s until the line went slack, and then retrieved using the reel. Before each cast, the unit was calibrated for 10 sec in the surface water. During each 1-hour collection period, at least 3 CTD casts were performed, one in each zone (as defined in §3.4).

Table 3 Sontek Castaway CTD Features (Sontek/YSI, 2012a)

Maximum Depth (m)	100
Salinity Accuracy (PSU)	±0.1
Temperature Accuracy (° C)	±0.05
Response Time (Hz)	5
Sampling Rate (Hz)	5

3.3 Transect 1 Study

The study site for the entire project is described in §2.3, but the analysis focus in Chapter 4 is on Transect 1, whose location in Galveston Bay is shown in Fig. 1; the Transect 1 location relative to Mid Bay Island is shown in Fig. 7. The Transect 1 data were collected from 0537 – 0641 hrs (UTC) on 6 August 2013 during peak ebb conditions and from 1237 – 1306 UTC on the same day during peak flood conditions. Fig. 8 shows the tidal elevation and wind information from the day before through the day after the data collection, obtained from NOAA at its Eagle Point NDBC buoy, the location of which can be seen in Fig. 2. During data collection, the wind was consistently out of the southeast with speeds ranging from 5-10 m/s. During the same periods, tidal elevation change is almost negligible. NOAA peak tidal current predictions for the study date are provided in Table 4. Limiting the data collection to 1 hour periods allowed tidal differences between transects to be neglected, unlike Buijsman and Ridderinkhof (2007), who had to correct for tidal elevation and current differences to average multiple transects. This approach also removed the need to account for changing environmental conditions, such as used by Reed et al. (2004). Transects can be treated as occurring simultaneously, and thus averaged for a clearer view of the mean water velocities during both peak ebb and peak flood conditions.

Table 4 NOAA Tidal Current Predictions for August 5^{th} to August 7^{th} at the Bolivar Roads near the mouth of Galveston Bay (NOAA, 2013c)

Date	Time (CDT)	Magnitude (kn)	Time (CDT)	Magnitude (kn)
August 5^{th}	05:07	+1.9	22:08	-1.6
August 6^{th}	05:39	+1.9	22:46	-1.5
August 7^{th}	06:02	+1.7	23:08	-1.3

Figure 7: Map of transect 1 near Mid-Bay Island.

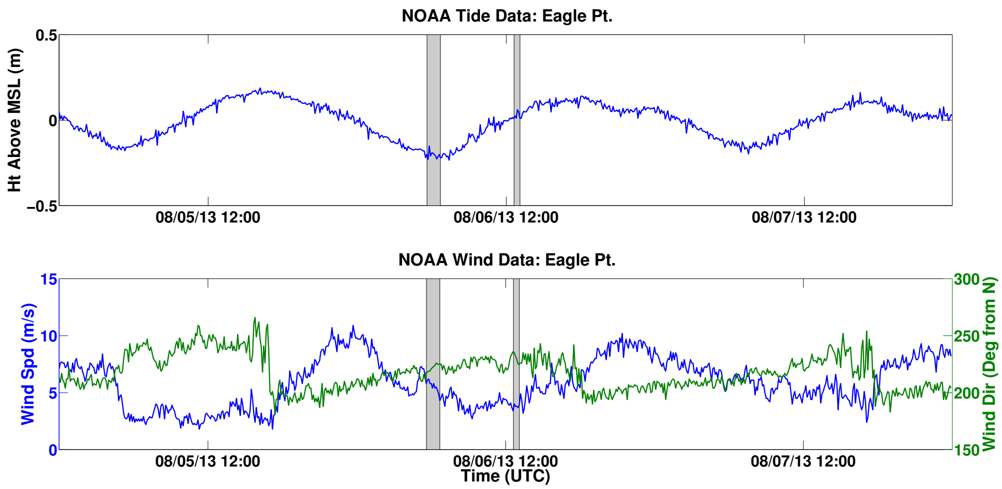

Figure 8: Tidal elevation (top) and wind (bottom) conditions for the time period of field study (`http://tidesandcurrents.noaa.gov/met.html?id=8771013`)

3.4 Data Analysis

The raw data from the ADCP are re-processed into along- and cross-channel velocities, conforming with the expected dominant flow directions. At Transect 1,the Houston Shipping Channel is aligned along an axis from 327° to 147°, where angles are measured from true north. The wind direction during the studies varies from 220° to 230°, and thus is predominantly a cross-channel effect. As a convention, velocities in the flood tide direction (heading towards 327°) are positive, whereas the ebb tide velocities (heading towards 147°) are negative. Convention for the cross-channel velocities are that northeasterly flows (heading towards Mid Bay Island at 57°) are positive and those towards the southwest (heading toward 237°) are negative. The data are processed as three separate zones based on observed similarities in both the bathymetry (Fig. 9) and the velocity data.

Zone 1 contains the shallow water (3-5 m depth) southwest of the Houston Shipping Channel, Zone 2 includes the water in the Houston Shipping Channel, and Zone 3 includes all shallow water between the Houston Shipping Channel and Mid-Bay Island. For each transect, the zonal water velocities were horizontally averaged, creating mean velocity profiles for each zone. Extraneous velocities were removed below the shallowest bottom depth measured in each zone by one of the 5 ADCP beams (i.e. the 0.5 MHz Echo-sounder beam and the 4 active transducer beams). Transects collected during ebb and flood flows were averaged separately. Standard deviation profiles were computed to illustrate velocity variability lost in mean profiles.

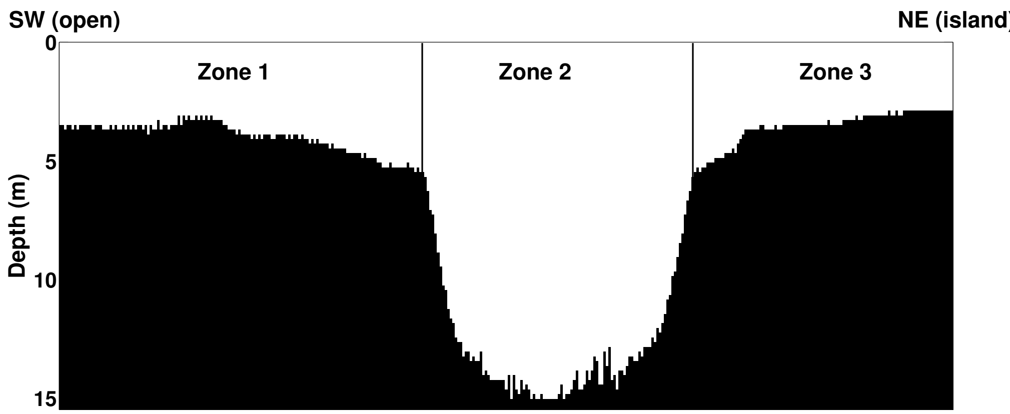

Figure 9: Profile view of transect 1 and definitions of Zones 1,2, and 3.

The raw ADCP data were exported from the SonTek RiverSurveyor files (.riv) to Matlab binary format (.mat files) through the RiverSurveyor software. A single Matlab file was created for each RiverSurveyor file exported. In the data export, the filename kernels were maintained and only the filename extensions changed. Organization of the exported data is found in Sontek (2012). Appendix C provides Matlab scripts and functions used to perform the data analyses.

Chapter 4 - Results and Discussion

4.1 Overview

Data are analyzed for peak flood and peak ebb conditions for in-channel velocities (Zone 2); upwind, open-water velocities (Zone 1), and downwind velocities (Zone 3) near Mid-Bay Island. Peak flood and ebb velocities in the channel were predominantly along the channel, with smaller cross-channel velocities occurring mostly at less than 4 m depth. The shallow regions upwind and downwind of the channel have significantly different behaviors. During flood, the upwind, open-water side (Zone 1) was fully mixed with a classic boundary-layer velocity profile in the positive (northwesterly) along-channel direction, and a slight negative (southwesterly) cross-channel component. In contrast the downwind, Mid-Bay Island side (Zone 3) during the flood was stratified with an along-channel velocity that, although also in the positive (northwesterly) direction, was approximately linear rather than following the classic boundary-layer shape. The corresponding cross-channel velocity had a negative (southwesterly) component that was weaker at mid-depth stronger near the bottom, indicating a near-bottom flow returning towards the channel. During peak ebb conditions, the upwind, open-water side (Zone 1) had stronger along-channel and weaker cross-channel velocities than the downwind side (Zone 3). The velocity variability downwind is larger than upwind for along-channel velocities during the ebb, likely indicating diverging flows near Mid-Bay Island.

4.2 Peak Flood Conditions

Fig. 10 shows along- and cross-channel velocities for each zone during peak flood tide. The along-channel surface velocities are similar in the channel (Zone 2) and near Mid-Bay Island (Zone 3), but are somewhat smaller in upwind, open water (Zone 1). Below the surface the profiles are significantly different. The in-channel (Zone 2) velocities are relatively uniform over depth with only small cross-channel components. However, the shallow Zone 1 and Zone 3 velocities are non-uniform, with differences more readily visible in Figs. 11 and 12.

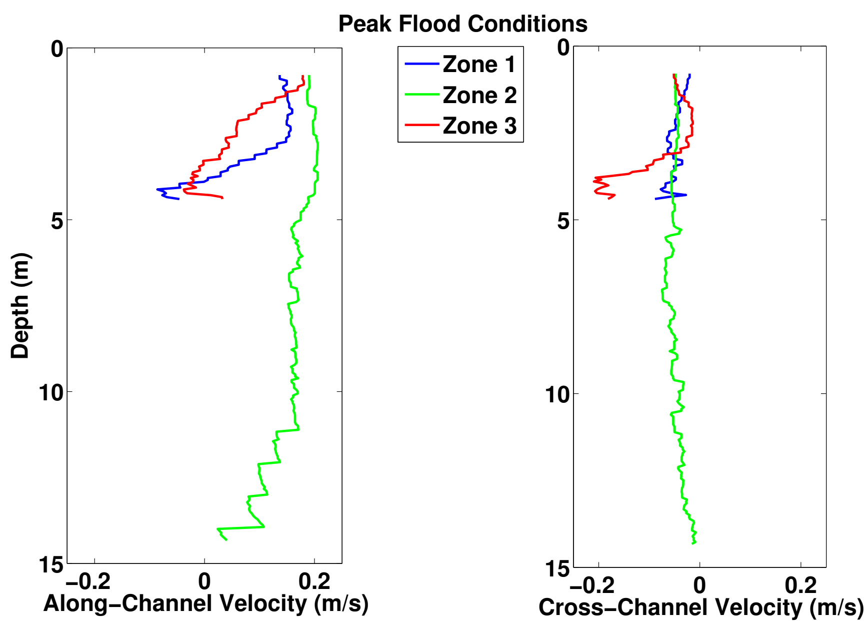

Figure 10: Average along- (left) and cross-channel (right) velocity profiles for each zone during peak flood conditions.

In open-water Zone 1, the velocity profile is consistent with uniform, unstratified open-channel flow (e.g. Henderson, 1969), which is expected for a tidally-forced open-water system. In contrast, a near-linear profile can be seen for Zone 3.

Cross-channel velocities, Fig. 12, indicate that open-water Zone 1 has an almost

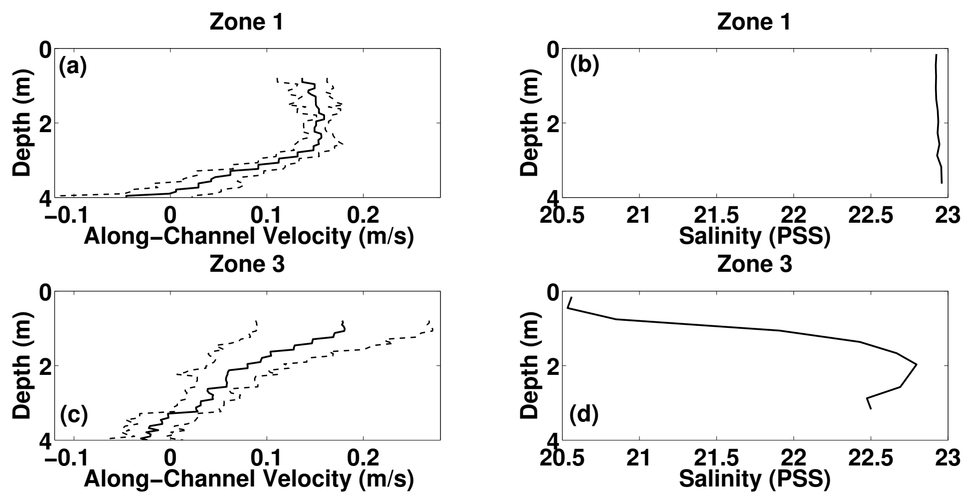

Figure 11: Flood along-channel velocity profiles with $\pm\sigma$ standard deviation lines for Zone 1 (a) and Zone 3 (c) and salinity profiles for Zone 1 (b) and Zone 3 (d).

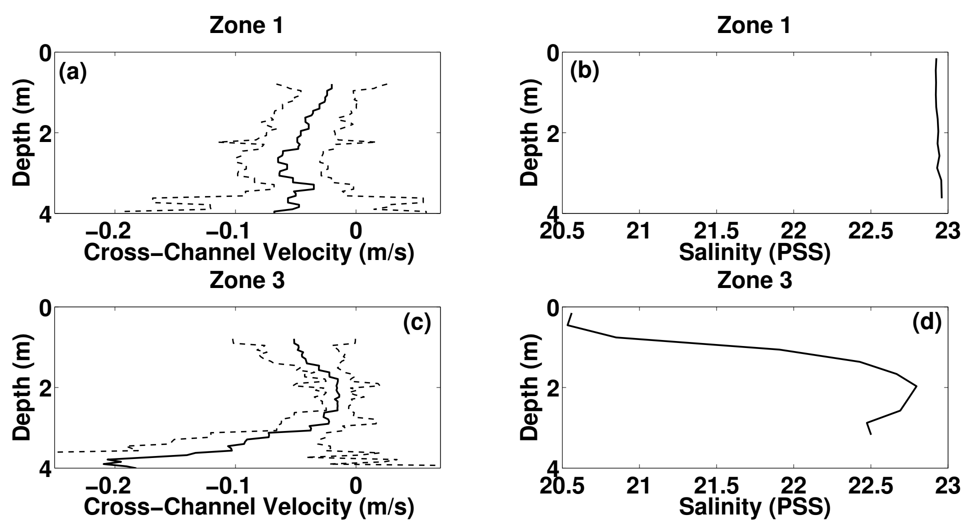

Figure 12: Flood condition cross-channel velocity profiles with $\pm\sigma$ standard deviation lines for Zone 1 (a) and Zone 3 (c) and salinity profiles for Zone 1 (b) and Zone 3 (d).

uniform component of roughly 0.06 m/s towards the southwest (negative), which is surprising because this direction opposes the wind, which was from the southwest throughout the flood tide data collection (Fig. 13). The tidal circulation is forcing a flow across the channel along a vector somewhat west of northwest; it is speculated that this result could be due to a large-scale flow divergence forced by Mid-Bay Island.

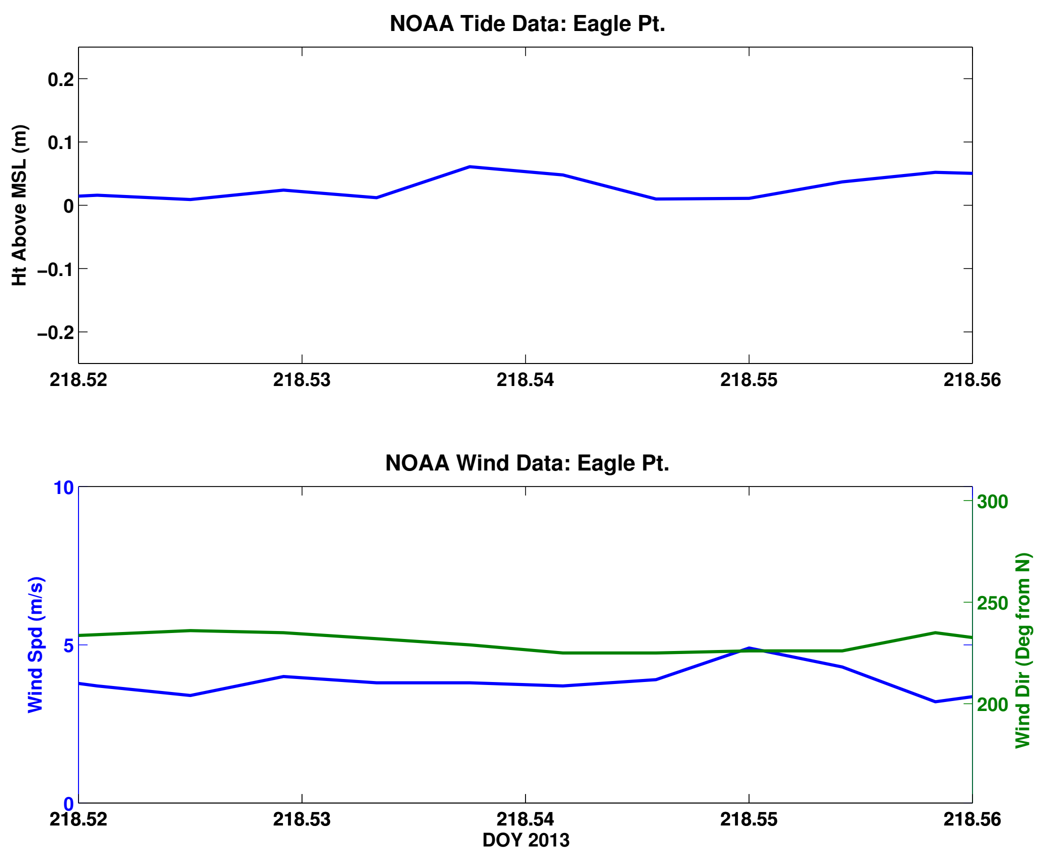

Figure 13: Tide (top) and wind (bottom) conditions for time period of peak flood current data collection

In Zone 3 near Mid-Bay Island, the approximately linear along-channel velocity (Fig. 11c) is accompanied by a cross-channel velocity (Fig. 12c) with a strong southwesterly (negative) flow along the bottom. This behavior appears to be related to stratification, which can be argued from Fig. 12b and 12d. In open-water Zone 1, the water is unstratified and the velocity profile similar to classic boundary layer theory; however the Mid-Bay Island Zone 3 shows salinity stratification, which appears to account for both the linear profile in Fig. 11c and the underflow in Fig. 12c. The source of the stratification cannot be determined from the data available.

Fig. 11d indicates that higher salinity water (and therefore more dense water) exists above lower salinity, or less dense, water in the lower 1 m near Mid-Bay Island (Zone 3). This density inversion cannot be stable, so it is either an undiagnosed instrument error or an effect associated with the instrument falling through a dynamically-mixing region. The instrument used to collect this data is new, with a sampling rate of 5 Hz and a fall rate of 1 m/s; thus, it is arguably capable of observing a dynamically mixing region with data points every 0.2 m.

Figures 14 and 15 show a representation of the hypothesized flow field for the upper 3 meters of the water column and the lower 1 meter of the water column, respectively. Fig. 14 indicates flow spreading outward from the island, with similar cross-channel velocities in all three zones. Fig. 15 shows the near-bottom flows in Zones 1 and 3 have lower magnitudes than near the surface, and that the cross-channel flow dominates in Zone 3 for near-bottom flow. Note there is a slightly negative along-channel component to the flow in Zone 3 that is consistent with Fig. 11c; this could be caused by stratification effects or a flow separation around the island. Further investigation is required to clarify this issue.

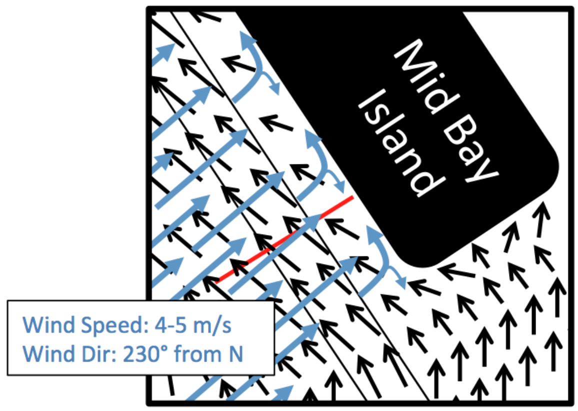

Figure 14: Representation of flow field for upper 3 meters of water column during peak flood conditions.

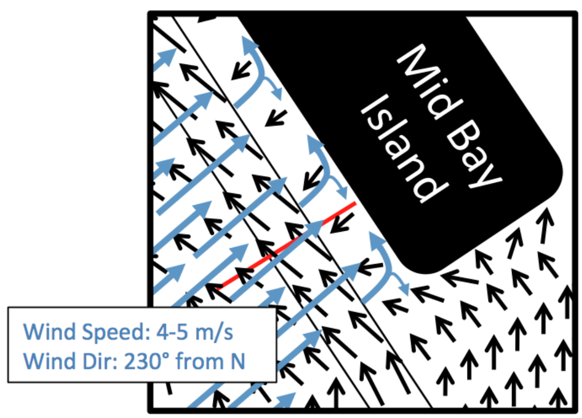

Figure 15: Representation of flow field for lower 1 meter of water column during peak flood conditions.

4.3 Peak Ebb Conditions

Fig. 16 shows along- and cross-channel velocity profiles for Transect 1 during peak ebb flows. Surface along-channel velocities in the channel (Zone 2) and open water (Zone 1) are above 0.17 m/s, whereas the mean along-channel velocity near Mid-Bay Island (Zone 3) is near zero. The in-channel (Zone 2) velocity profile over the entire depth is similar to classic boundary layer profiles. The cross-channel velocities in Zone 2 are only interesting in the upper 4 m, where they are similar in profile, but offset from, cross-channel velocities in shallow Zones 1 and 2.

The difference between the along-channel surface velocities in the open water (Zone 1) and near the island (Zone 3) indicate the island affects the flows in a way not evident during flood flows (Fig. 10). A possible cause is the location of Transect 1 relative to the chain of dredge spoil islands. For flood flows, the transect is close to the leading edge of the first of the dredge spoil islands, in what could be considered a developing horizontal boundary layer. In contrast, for the ebb flows the transect is at the far end of the last of the series of dredge spoil islands (relative to the flow), i.e. well back from the leading edge of a horizontal boundary layer along the islands.

Details of the velocities in open-water (Zone 1) and near Mid-Bay Island (Zone 3) are shown in Figures17 and 18. The large variability in the along-channel velocity (relative to the mean velocity) close to Mid-Bay Island indicates a region of active turbulence, particularly compared with the more typical velocity profile in open water. Figures 17b and 17d show salinity stratification for both Zone 1 and Zone 3. Zone 1 shows a potential density inversion similar to Zone 3 during peak flood

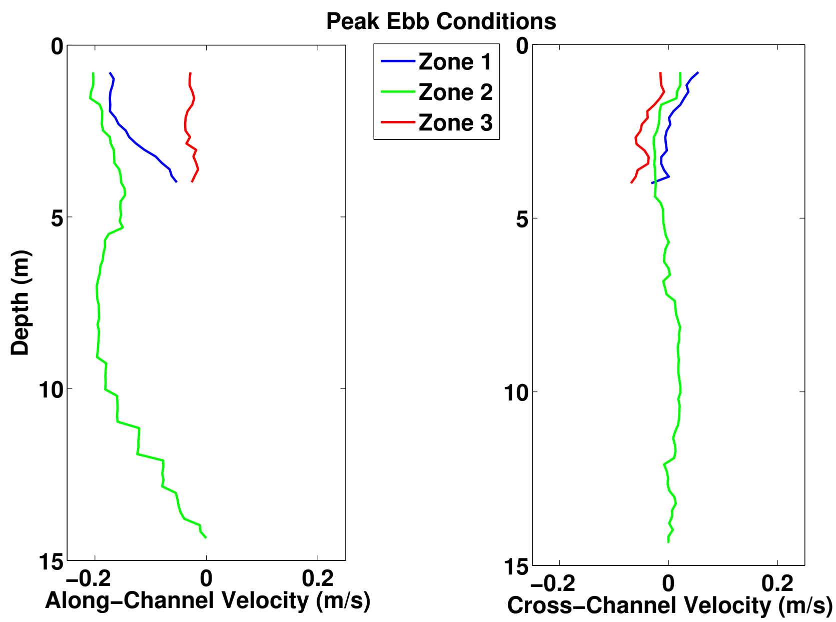

Figure 16: Average (a) along- and (b) cross-channel velocity profiles during peak ebb conditions.

conditions. The cross-channel velocity profiles for Zone 1 and 3 (Fig. 18) have similar shapes, but different magnitudes. During the ebb tide, the wind was $215° - 220°$ from north (Fig. 19) or about $68° - 73°$ from the channel, providing a significant cross-channel component and a smaller component opposing the along-channel ebb tide. The wind stress opposing a displacement driven by the boundary layer along the dredge spoil islands may account for the profile shapes in Fig. 18 that show a greater wind influence (increasingly northwesterly velocity) further from the island.

Fig. 20 illustrates how the broader flow field near the island might look during ebb conditions. Similar to Fig. 14, the flow is shown spreading out around Mid-Bay Island, inducing a cross-channel flow in all three zones. The highest cross-channel flow is shown nearest to the island in Zone 3, and the lowest cross-channel flow is shown furthest from the island in Zone 1.

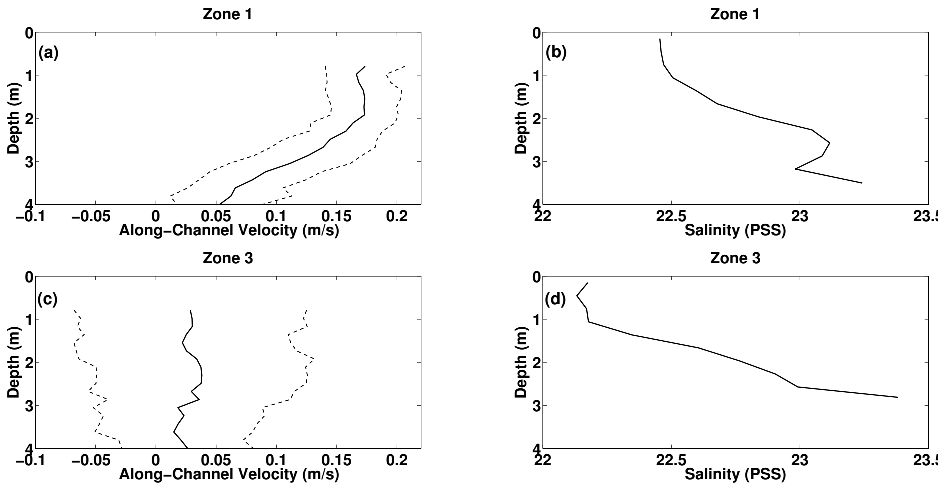

Figure 17: Ebb along-channel velocity profiles with $\pm\sigma$ standard deviation lines for Zone 1 (a) and Zone 3 (c) and salinity profiles for Zone 1 (b) and Zone 3 (d).

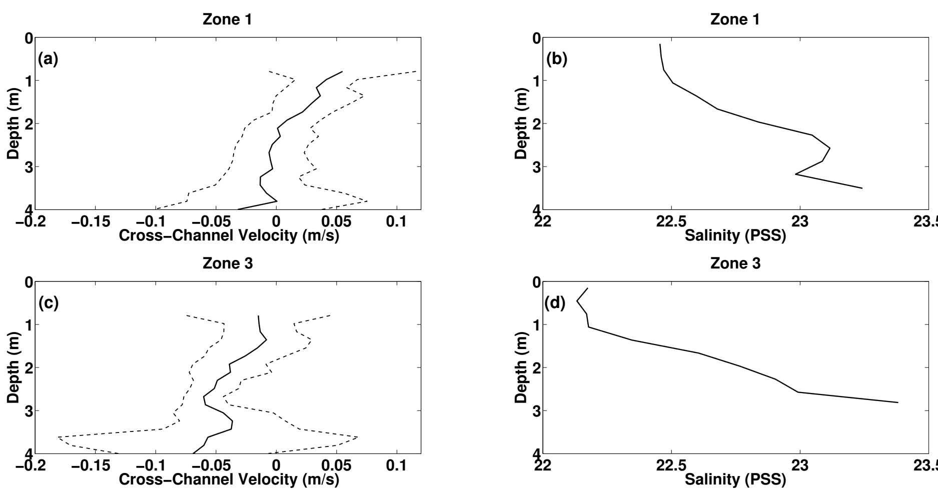

Figure 18: Ebb condition cross-channel velocity profiles with $\pm\sigma$ standard deviation lines for Zone 1 (a) and Zone 3 (c) and salinity profiles for Zone 1 (b) and Zone 3 (d).

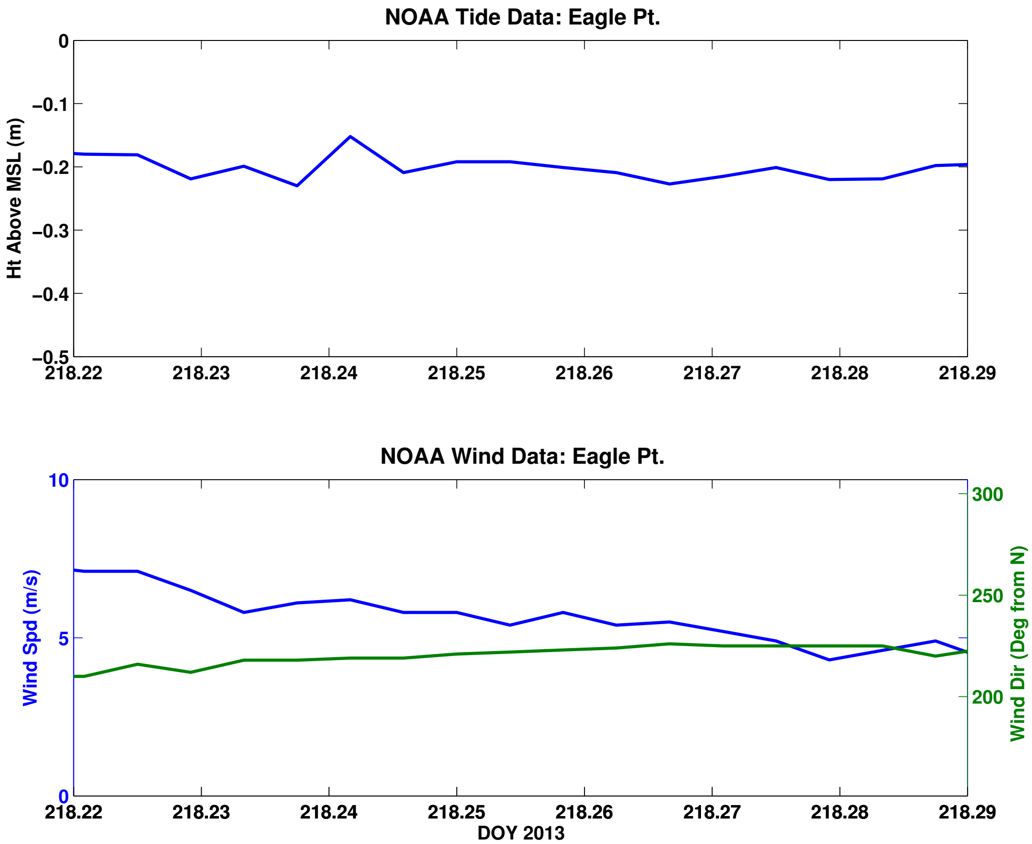

Figure 19: Tide (top) and wind (bottom) conditions for time period of peak ebb current data collection

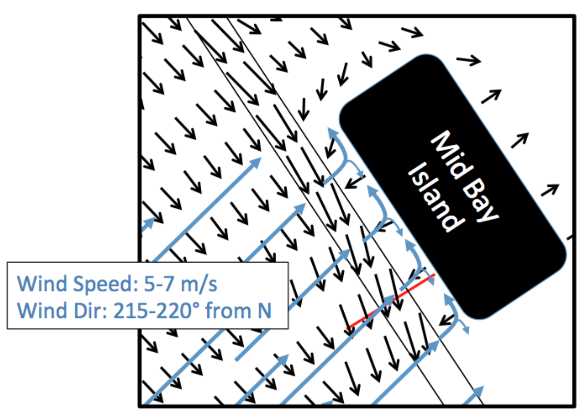

Figure 20: Representation of flow field during peak ebb conditions.

Chapter 5 - Conclusions and Future Work

5.1 Conclusions

This study focused on flow patterns near Mid-Bay Island, a dredge spoil island in Galveston Bay near the Houston Shipping Channel (located at 29° 34' 37.30" N 94° 55' 03.44" W). Previous studies have either focused exclusively on in-channel flow or used a bay-scale circulation model that did not capture the effects of islands with a relatively small footprint such as Mid-Bay Island. Winds of 5-7 m/s at 215-230° from N were present during data collection. For both peak ebb and flood conditions, the tidal circulation forced flow in a direction opposing the wind, perhaps due to a large-scale flow divergence forced by Mid-Bay Island. The strongest such currents were measured closest the island.

During peak flood flow, the shape of the along-channel velocity profile for the open water upwind of the channel at Mid-Bay Island indicated uniform flow, and the salinity profile indicated a well-mixed water column. The near-island along-channel velocity profile showed a near-linear trend, and the salinity profile indicated a stratified water column. This suggested that the stratification had some effect the velocity profile shape, but further research is needed to better quantify this effect.

During peak ebb flow, the near-island along-channel velocities were highly variable with respect to the mean velocity, indicating an area of active turbulence. Salinity profiles collected in the open water and near-island both showed stratification, something that was not seen during flood conditions.

Differences in observations between flood and ebb flows can possibly be attributed to the survey location with respect to the chain of dredge spoil islands. During flood flows Mid-Bay Island is the first of the islands, and the flows surrounding the island may part of a developing horizontal boundary layer. During ebb flows the island is last in the chain relative to the direction of flow, and therefore the surrounding flows are well back from the leading edge of a horizontal boundary layer.

5.2 Future Work

Further work is needed to better characterize and quantify the flow around Mid-Bay Island. The data presented in this report was collected along one transect over a relatively short time period. Thus, it is difficult to separate effects caused by meteorological factors (*e.g.* wind from the tidal forcing). Furthermore, the horizontal spatial variability in the velocity field likely changes both through the dredge spoil islands and in the open water. Future studies should include data collected over a variety of wind conditions, as well as data collected along multiple transects over a broader area.

Appendices

A Field Reports

This appendix includes field reports for each field trip to Galveston Bay.

Galveston Bay: Day Trip Report

(All times reported in C.D.T.)

On 04/07/2013, Prof. Ben Hodges, David Christiansen, and Abigail Tomasek left the Center for Research in Water Resources at ~6:30 A.M. on a field trip to Galveston Bay, TX. The purpose of the trip was to collect some preliminary velocity data in various locations of the bay. The survey equipment used included a Sontek/YSI HydroSurveyor M9 unit attached to the side of a 23-foot, fiberglass flat bottom boat with a custom-made PVC and aluminum mounting arm. The boat had a 150 horsepower, two-stroke engine that currently has trouble maintaining speed at velocities exceeding 6-7 knots.

The boat was launched at Eagle Point Fishing Camp in San Leon, TX at 11:35 A.M., and a compass calibration of the M9 unit was successfully completed. A transect from Eagle Point to Smith Point was then run. The transect did not span all the way to Smith Point, but stopped shortly after passing "Bird Island" on its southern side. The water between Bird Island and Smith Point is only 1-5 feet deep, so if this area is to be surveyed in the future it should be done during high tide. The weather was sunny and warm, with a fairly strong wind out of the south-by-southeast, causing 1-1.5 foot waves. A steady speed of 5-6 knots was maintained for most of the transect. The return transect was run parallel to the first, but dipped as far as 1 km south where it crossed the Houston Ship Channel. Both transects took a

Next, a velocimetry survey was conducted along and across points of the Houston Ship Channel. This survey began with a transect across the ship channel at approx. 29°30'45" N, 94°52'45" W, which was followed by an along channel survey steaming at 4-5 knots northward for 2.58 km. At that point a large tanker named Agapi S was coming into port and a tug and barge was leaving port. Another cross-section transect was taken at 3:18 P.M. passing behind the tug and barge (see photos for proximity). The Agapi S was then allowed to pass, at which point three more transects were completed (between reference points 59 and 60): the first being directly behind the Agapi S and the next two at increasing distances from Agapi S (again, see photos for proximity). The purpose of these transects was to identify the dissipation and behavior of ship wakes in a ship channel. The along-channel survey was then continued for another 3 km, after which an approaching tug and barge forced the survey out of the ship channel. At this point, the survey was continued at a due north trajectory towards a rip-rap-lined dredge spoil island. The survey passed along the southern point of the island and then turned back across the channel, completing three more transects. The first of these transects was run in line with the southeastern edge of the spoil island. The second passed through a dissipating ship wake at 4:08 P.M. and crossed the channel 0.4 km north of the first (Stolt tanker). The third transect, which was 0.33 km north of the second, passed through a dissipating ship wake at 4:16 P.M. (BBC tanker).

The along-channel survey was then continued for 1.15 km southward until high waves caused the team to leave the channel and head back to the dock at Eagle

Point. Data was collected along the ~7 km long line back to shore, and the survey was terminated at 5:03 P.M. once the dock was reached.

15 gallons of fuel was consumed during the survey, and the boat speed was held between 4-8 knots for its entirety. During the last 7 km line the speed was oscillating between 5 and 8 knots due to motor problems for the first 3-4 km, after which the speed was reduced to 6.5 knots to reduce motor surging.

Field Trip Report – 6/19/13 to 6/21/13

6/19/13

Left CRWR at 8:45 am, got to Eagle Point Fishing Camp around 1:30 pm. Loaded and launched boat, then calibrated the ADCP compass just outside the EPFC entrance. Lowrance GPS unit was not locating us properly (WILL TRY THE BUCKET ONE NEXT TRIP). We headed for Spoil 2 (as closely as we could locate it). As we approached the southern edge of the spoil island, we decided that crossing the shipping channel at the marker set 67-68 would be an appropriate spot to capture the restricted flow along the western edge of the island in both max ebb and max flood velocity conditions. When we were about to start measurement, it was pointed out that the computer was not charging and was nearly dead. After some investigation, the problem turned out to be the wiring in the battery cooler. Several attempts at rewiring proved useless, so we headed back to the dock. No data was collected. A trip to Home Depot was made and new ring connectors purchased. The battery cooler was rewired in the parking lot and is currently functional. We also constructed and installed the Bimini cover. We stayed at the Holiday Inn Express in Kemah, where they made accommodations for us to stay at the government rate.

6/20/13

We launched from EPFC around 10 am. The ADCP compass was calibrated, and we began data collection just south of the determined transect perpendicular to the western edge of the island. Using the two markers as a guide, we drove along the edge of the island until we were aligned with them, at which point we turned west and steamed at 4.5 knots SW in line with markers 67-68. This heading was maintained through the shipping channel and once we were past marker 67, we changed course slightly to aim for "Brown Abandoned Oil Rig" (See Google Earth) and stopped when we drew even with "Yellow Abandoned Oil Rig" (again, see Google Earth). This transect was repeated 3 times going east to west and twice going west to east. CTD casts were performed 2 times outside the shipping channel at 11:30 am and once inside the channel at 11:40. We then followed a container ship south in the channel to provide a smoother, albeit smoggier trip.

With the absence of a working GPS unit, which housed the coordinates for the open transect, we selected the marker pair of 45-46 to use as guides. Beginning to the east of the channel, we drew even with a small platform to our north, aligned ourselves with the markers, and steamed at 4.5 knots to the west through the channel and on out into the shallow water, stopping to turn around near 29 27' 58" N, 94 51' 28" W. This transect was repeated 3 times in each direction, during the last of which the software became nonresponsive and was closed. It became uncertain whether this data had been lost or not, so it was decided to perform the transect 3 more times in the west-east direction and twice more in the east-west direction, creating a new session between each to prevent any data loss due to software error. CTD casts were performed at the beginning and end of this 2-hr run, both in and out of the channel.

We packed up and continued south along the channel until we reached the Texas City Channel near channel markers 25A and 25. Unsure of what eastern point to steam towards and without a GPS unit, we moved to the eastern endpoint of the mouth transect and chose a red intracoastal channel buoy off the southern shore of a barrier island as Mouth 2 near 29°22'29.41"N, 94°46'59.26"W. Steaming from this point westward at 4.5 knots, we kept our heading towards the Texas City Dike at 29°21'47.65"N, 94°48'37.81"W. This transect was repeated twice in each direction. Dolphins came very close to the ADCP during the first east-west transect, and can actually be seen in the data as sharp spikes in vertical beam range as they passed under the unit to inspect it. This occurred only on this transect. Again CTD casts and point measurements were taken at the beginning and end of the 4-transect run, outside the channel at the beginning and both in and outside the channel at the end.

The equipment was then secured and we made for EPFC, which took almost an hour to reach through rough waters. It was suggested that next time we launch from EPFC for the two northern locations, and return to dock and drive south to launch from the Texas City Dike boat ramp for the Mouth transect. Doing this should save time and unnecessary wear and tear on the boat.

After closer inspection of the current predictions, as well as the discovery of a NOAA Houston Shipping Channel model, it appears that future trips should plan to collect data no earlier in the day than 3 pm, and that collecting data in the early morning should prove worthwhile (providing we have working GPS and lights). This is demonstrated in the data collected on 6/20 at the Spoil and Open locations, which both show velocities less than 30 cm/s everywhere in the channel.

6/21/13

Because of the revelations of the previous day, data collection was not started until just after 3 pm. After compass calibration, the open transect was run first, 3 times in both the east-west and west-east directions. CTD casts and point measurements were taken on either side of the channel, as well as in the channel. It should be noted that the included string in the CTD kit was not long enough to reach the bottom of the shipping channel, and a longer cord will have to be purchased for future trips. Garrett suggested braided fishing line. The survey then moved to the spoil transect, which was run 6 times total: 3 in either direction, and CTD casts and point measurements were taken. Ship traffic was lighter this day, and all transects were performed well after any ships moved through the channel. A NOAA/TAMU technical report was located which includes analysis of CTD/ADCP data in Galveston Bay from 1999. This report includes data from a transect performed between the same two channel markers as the spoil transect. However, the spoil island did not exist at that time, so it may be interesting to compare data from their transect with ours.

Galveston Bay: 7/1/13 – 7/3/13

Day 1: Max Ebb Cycle

After arriving at Eagle Point Fishing Camp (EPFC) around 5 pm, loading up the boat and launching, we drove south towards the mouth through rough waters. It was decided that future data collection sessions would begin at the Texas City Dike, where we would launch, collect 2 transects across the mouth of the bay, and return before driving up to EPFC, launching, and collecting data at the remaining two transects. This initial struggle caused us to fall well behind schedule later in the night. We began collecting data 1 hour after peak ebb currents began (07/01/2013 23:55 UTC). Two transects were completed, one in each direction, in roughly an hour (ended at 07/02/2013 00:52 UTC). CTD casts were performed near the point Mouth W, in the shipping channel along the transect, and near Mouth E. The details of these casts can be seen in the table below. We then moved north in the shipping channel until we reached the Open Water transect (channel markers 45 and 46). This transect was performed 6 times in the next hour, but the data for these transects did not record. Our theory is that when the screen was frozen except for the time counter, the data was not recording. Regardless, CTD casts were performed near points Open E, Open W, and in the shipping channel along the Open Water transect. The details of these casts are outlined in the table below. We then continued north in the shipping channel until we reached the southwestern point of the spoil island near channel markers 67 and 68. At 04:47:33 UTC on 07/02/2013 the first transect was started near Spoil W. This transect and 5 more were completed over the next hour. After looking at the data and a time series plot of measured currents at the mouth of the bay, it was noted that the velocities collected at this time were very low, but perhaps still useful to the study. CTD casts were taken, the details of which can be seen in the table below. This ended the maximum ebb current session. Once we returned to EPFC and loaded the boat on the trailer, it was already time for the maximum flood currents to be present near the Mouth transect. It was decided that this session would be skipped, and we returned to the hotel for the night.

Day 2: Max Ebb Cycle

We arrived at the boat ramp on the Texas City Dike (TCD) and were on the water collecting data at 22:37:21 UTC on 07/02/2013 near Mouth W. Two transects were completed in the next hour, including CTD casts at both Mouth W and Mouth Channel. We then returned to the boat ramp, loaded up, and drove to EPFC, where we launched and drove to the Spoil Island transect. Over the next hour, 6 transects were completed, and CTD casts were collected at Spoil W, Spoil E, and Spoil Channel. Refer to the table for details of these casts. From here we traveled south via the shipping channel to the Open Water transect. 6 transects were completed over the next hour, but only 3 recorded any data. It is believed that the frozen software was again the cause for this data loss. CTD casts were collected at Open E, Open W and Open Channel, the details of which can be seen in the table below. With the maximum ebb cycle completed, we returned to EPFC, where we loaded the boat and drove into Kemah for a short break before heading south to begin the maximum flood cycle.

Day 2: Max Flood Cycle

We arrived at Mouth W around 07:45 UTC, and began the first of two transects at 07:59 UTC 07/03/2013. However, a large container ship obstructed our path across the channel. So the transect was abandoned. Because of equipment damage, our computer was unable to charge and only had roughly 20 minutes of battery life. This allowed for one full transect and a partial transect across the shipping channel only. This data was collected just north of Mouth transect, as seen in the figure below. Once the computer died, 2 CTD casts were collected: one near the boat's location in the figure below and one in the shipping channel just north of the Mouth transect. We then returned to TCD and drove to Walmart to purchase a new charger for the computer. After returning to EPFC, it was discovered the boat

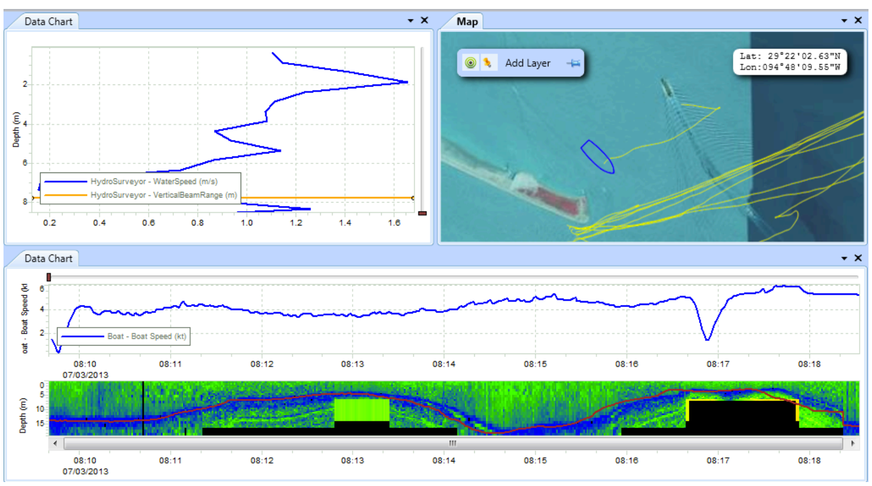

Figure 1: Location and depth profiles of partial transects near Mouth W

motor batteries were dead. After dealing with this issue, we were able to get back on the water and to the Open Water transect at 12:49 UTC on 07/03/2013. Because of the time lost dealing with the previously discussed issues, it was decided that data would be collected at Open Water and Spoil Island for only a half hour each (3 transects at each). Only 2 of the 3 transects recorded at the Open Water location, and an error occurred with the recorded boat speed over the first transect at this location as well. CTD casts were collected near Open W and Open Channel, and we took a more direct route from Open Water to Spoil Island. This saved roughly 10 minutes compared to staying in the shipping channel. Three transects were completed at Spoil Island without incident, and CTD casts were collected near Spoil W, Spoil E, and Spoil Channel. This completed the max flood cycle, and the trip.

Galveston Bay: 7/17/13 – 7/19/13

Crew: David Christiansen, Garrett Kehoe, Matt Rayson

Day 1: Max Ebb Cycle

We arrived at the Texas City Dike boat ramp at 16:41, and had the boat set up at 17:03. After dealing with a slight battery issue, we were able to get on the water at 17:24. Matt was running slightly late, so Garrett and I went on ahead with data collection. After calibrating the unit, two Mouth transects were completed, the second of which was not properly recorded by HydroSurveyor (HS), which has been attributed to the software's incompatibility with Windows 8. CTD casts were taken at either endpoint and in the channel. The details of all CTD casts and ADCP transects can be found in the tables provided at the end of this document.

Once back on land, we packed up the boat, and with Matt following, headed to EPFC at 6:50. After setting the boat up, we launched at EPFC, where we lost the first of two trailer tires pulling the trailer back out of the water. We got back on the water and began collecting data at Spoil W at 20:33. Six Spoil transects were completed during the max ebb cycle, and CTD casts were completed at either endpoint and in the center of the channel. This concluded the Day 1 max ebb cycle. *Note: Second trailer tire was lost pulling boat out of water after Spoil Island data collection.

Day 2: Max Flood Cycle

Our limited mobility caused us to decide to forgo any more Mouth transects. Instead we decided to collect more data at Spoil Island. Eight full transects were completed, and supporting CTD casts were taken at all three previously discussed locations.

Day 2: Max Ebb Cycle

The next morning we located a full service boat shop, which gave us a quote for the trailer repair, and suggested we use a boat ramp under the bridge in Kemah, TX approximately ¾ mile from the hotel until our trailer is repaired. From here it was suggested by Matt that we take a long transect from Clear Lake, which is known for its low turbidity, out into the open bay (Spoil E was used as an endpoint). CTD casts were collected every ¼ mile along the transect, with the goal of capturing the horizontal salinity gradient. Once we arrived at Spoil E, 7 additional transects were collected at Spoil Island before heading back to Kemah.

Day 3: Max Flood Cycle

After a short break, we launched again from Kemah and at 1:09 began our second Clear Lake to Spoil E transect. The waves that night were 2-3 ft, which made the going much rougher than the day before. I believe the additional shaking caused the computer to disconnect from the M9 unit about 1 hour and 20 minutes into the transect. We collected CTD casts every ½ mile along this transect. The computer problems were noticed ~4 minutes after they occurred, and the devices were reconnected and the transect continued. Once we arrived at Spoil E, 5 more transects were completed and CTD casts were done at Spoil E, W and Channel.

Galveston Bay: 8/05/13 – 8/07/13

Crew: David Christiansen, Garrett Kehoe

Day 1: Max Ebb Cycle

We got to Texas City Dike launch site and out on the water by 21:30 CDT on 08/05. The winds were out of the south and boat traffic was fairly high. This was the first time using RiverSurveyor with the mobile device. The switch was made from HydroSurveyor on the advice of a Sontek technical advisor, based on the fact that HydroSurveyor was not yet compatible with Windows 8. Two Mouth transects were completed. Going back out from Mouth W to collect a CTD cast in the channel, we decided to collect ADCP data, so there is a third, partial transect from Mouth W to the east side of the channel. CTD casts were performed at each end of the transect and in the Houston Shipping Channel. We then packed up and drove to Kemah. It was decided during the last trip that it would save time to launch from the Kemah Bridge and steam southeast to Mid-Bay Island rather than driving to Eagle Point Fishing Camp and steaming northeast to the island.

After launching from the Kemah Bridge around 00:00 CDT, we headed from the entrance of Clear Lake to Spoil W. The water was much calmer than last trip. We arrived at Spoil W and began running transects. During the first transect, we turned around in the middle of the channel to avoid being trapped against the island with a tanker (and its subsequent wake) approaching. 7 transects were completed. An eight was attempted, but another approaching tanker caused us to turn around early. This transect includes data from Spoil W to channel marker 68. A final, full transect was collected, during which we passed approximately 10 seconds behind two tugs and barges, one heading each direction in the channel.

Day 1: Max Flood Cycle

After a quick break, we arrived at the Texas City Dike at 04:53 CDT. Though the tidal predictions said the max flood currents should occur at 05:40 CDT, checking GBOFS caused us to head out earlier. Two Mouth transects were completed, during one of which we were forced slightly north to avoid a tug and barge. CTD casts were collected at each endpoint and in the channel. We then headed back north to Kemah.

We arrived again at Spoil W and collected 6 transects. During the last one, we passed about 1 minute behind two tankers. At 08:21 CDT, we headed back to Kemah, having collected CTD cast data at Spoil W, Spoil E, and in the channel.

Day 2: Max Ebb Cycle

The second day found us at Texas City Dike and on the water around 22:00 CDT. Unfortunately, as we began to calibrate the compass of the ADCP, an error was reported. After wrestling with the software and M9 unit, we were forced to call off the Mouth transects. Attempting to salvage Day 2, we reattempted the calibration at Kemah Bridge, to no avail. After talking to Sontek technical assistance, it was decided to end the trip early. We headed back to Austin, and sent the M9 unit to Sontek for repairs.

B Data Summary

File Name	# of Transects	Location	Notes
20130407_164551	2	-	Eagle Pt to Smith Pt and back
20130407_193238	6	-	Several 'wake' transects, up the channel, several transects near Mid-Bay Island

Figure 21: ADCP Data Summary for 04/07/2013 Trip

File Name	# of Transects	Location	Notes
20130620_152016	5	Spoil	
20130620_174231	nothing		
20130620_174431	6	Open	
20130620_184300	1	Open	
20130620_185017	1	Open	
20130620_185806	1	Open	
20130620_190615	1	Open	
20130620_191358	1	Open	
20130620_201634	1	Mouth	
20130620_204154	1	Mouth	
20130620_210407	1	Mouth	
20130620_212705	nothing		
20130620_212835	1	Mouth	
20130621_203428	1	Open	
20130621_205040	1	Open	
20130621_205957	1	Open	
20130621_210857	1	Open	
20130621_211640	1	Open	
20130621_212513	1	Open	
20130621_222030	1	Spoil	
20130621_223215	1	Spoil	
20130621_225024	nothing		
20130621_225044	1	Spoil	
20130621_225803	2	Spoil	

Figure 22: ADCP Data Summary for 06/19/2013 Trip

File Name	# of Transects	Location	Notes
20130701_235546	1	Mouth	
20130702_002142	nothing		
20130702_002559	1	Mouth	
20130702_022423	nothing		
20130702_023506	nothing		
20130702_024455	nothing		
20130702_025936	nothing		
20130702_030822	nothing		
20130702_031614	nothing		
20130702_044732	1	Spoil	
20130702_045355	1	Spoil	
20130702_050002	1	Spoil	
20130702_051714	1	Spoil	
20130702_052514	1	Spoil	
20130702_053147	1	Spoil	
20130702_223721	1	Mouth	
20130702_225810	1	Mouth	
20130703_013819	1	Spoil	HS shows WaterSpeed at 2-3 m/s
20130703_014516	1	Spoil	
20130703_015201	1	Spoil	
20130703_015749	1	Spoil	
20130703_020353	1	Spoil	
20130703_020957	1	Spoil	
20130703_032449	nothing		
20130703_033530	nothing		
20130703_034219	nothing		Displays in HS, Devices malfunctioned during transect
20130703_035002	1	Open	Start of transect shown as 03:50:46
20130703_035832	nothing		
20130703_040447	nothing		
20130703_040520	nothing		
20130703_041251	nothing		
20130703_041301	1	Open	Displays in HS, Devices malfunctioned during transect
20130703_075910	nothing		
20130703_080938	1	Mouth	Just channel, north of other Mouth transects
20130703_124902	1	Open	Device malfunction over channel
20130703_125752	1	Open	
20130703_135531	1	Spoil	
20130703_140200	1	Spoil	
20130703_140904	1	Spoil	

Figure 23: ADCP Data Summary for 07/01/2013 Trip

File Name	# of Transects	Location	Notes
20130717_223535	1	Mouth	
20130717_230412			
20130718_013308	1	Spoil	
20130718_014420	nothing		
20130718_015454	1	Spoil	
20130718_020256	1	Spoil	
20130718_021410	1	Spoil	
20130718_022254	1	Spoil	
20130718_023243	nothing		Large wake against island
20130718_023626	1	Spoil	
20130718_071944	nothing		
20130718_072243	1	Spoil	
20130718_073034	1	Spoil	
20130718_074333	1	Spoil	
20130718_080013	1	Spoil	
20130718_080645	nothing		
20130718_081942	1	Spoil	
20130718_082829	1	Spoil	
20130718_083851	2	Spoil	
20130719_001355	8	Spoil	Began in Clear Lake
20130719_060600	nothing		
20130719_061043	nothing		Began in Clear Lake, device malfunctioned ~halfway to channel
20130719_073313	6	Spoil	One wide transect indicates CTD cast taken in channel. Last transect looks questionable in HS

Figure 24: ADCP Data Summary for 07/17/2013 Trip

File Name	# of Transects	Location	Notes
20130805213304.riv	1	Mouth	
20130805220231.riv	1	Mouth	
20130805222546.riv	1	Mouth	Only Mouth W to other side of channel
20130806003705.riv	1*	Spoil	Had to turn around in middle of SC to avoid being trapped against Spoil Island w/ large ship coming
20130806005105.riv	1	Spoil	
20130806005710.riv	4	Spoil	
20130806012407.riv	2	Spoil	Started at Spoil W, went to E marker and turned around to avoid being trapped against island
20130806014109.riv	1	Spoil	Transect passed ~10 sec behind t&b going S and t&b going N
20130806050816.riv	2	Mouth	Changed course N slightly to avoid t&b
20130806073730.riv	5	Spoil	
20130806080609.riv	1	Spoil	
20130807104931r.rivr	nothing		File from night of compass malfunction

Figure 25: ADCP Data Summary for 08/05/2013 Trip

Cast Number	Device	Cast Time (Local)	File Name	Number of Samples	Location Source	Sample Type	Notes
1	CC1317002	6/20/13 11:34	CC1317002_20130620_163411	697	GPS	Cast	
2	CC1317002	6/20/13 11:37	CC1317002_20130620_163719	302	GPS	Cast	
3	CC1317002	6/20/13 11:42	CC1317002_20130620_164249	337	GPS	Cast	Did not reach channel bottom (reached ~10 m depth)
4	CC1317002	6/20/13 11:44	CC1317002_20130620_164439	140	GPS	Point Measurement	
5	CC1317002	6/20/13 11:45	CC1317002_20130620_164558	344	GPS	Point Measurement	
6	CC1317002	6/20/13 12:38	CC1317002_20130620_173844	253	GPS	Cast	
7	CC1317002	6/20/13 12:39	CC1317002_20130620_173949	116	GPS	Point Measurement	
8	CC1317002	6/20/13 14:27	CC1317002_20130620_192752	384	GPS	Cast	
9	CC1317002	6/20/13 14:31	CC1317002_20130620_193101	304	GPS	Cast	Did not reach channel bottom (reached ~12 m depth)
10	CC1317002	6/20/13 14:32	CC1317002_20130620_193223	113	GPS	Point Measurement	
11	CC1317002	6/20/13 15:14	CC1317002_20130620_201423	171	GPS	Cast	Closer to shore than other cast at Mouth E
12	CC1317002	6/20/13 15:15	CC1317002_20130620_201512	143	GPS	Point Measurement	
13	CC1317002	6/20/13 16:27	CC1317002_20130620_212742	139	**none**	Point Measurement	
14	CC1317002	6/20/13 17:05	CC1317002_20130620_220506	310	GPS	Cast	Did not reach channel bottom (reached ~9 m depth)
15	CC1317002	6/20/13 17:06	CC1317002_20130620_220659	265	GPS	Cast	Did not reach channel bottom (reached ~11 m depth)
16	CC1317002	6/21/13 15:28	CC1317002_20130621_202805	258	GPS	Cast	
17	CC1317002	6/21/13 15:29	CC1317002_20130621_202924	174	GPS	Point Measurement	
18	CC1317002	6/21/13 16:35	CC1317002_20130621_213517	124	GPS	Point Measurement	
19	CC1317002	6/21/13 16:36	CC1317002_20130621_213603	240	GPS	Cast	
20	CC1317002	6/21/13 16:42	CC1317002_20130621_214259	94	GPS	Point Measurement	
21	CC1317002	6/21/13 16:43	CC1317002_20130621_214329	248	GPS	Cast	Did not reach channel bottom (reached ~9 m depth)
22	CC1317002	6/21/13 17:29	CC1317002_20130621_222914	117	**none**	Point Measurement	
23	CC1317002	6/21/13 17:30	CC1317002_20130621_223042	0	GPS	**Invalid**	
24	CC1317002	6/21/13 17:30	CC1317002_20130621_223054	140	GPS	Point Measurement	
25	CC1317002	6/21/13 18:13	CC1317002_20130621_231342	114	GPS	Point Measurement	
26	CC1317002	6/21/13 18:14	CC1317002_20130621_231435	162	GPS	Cast	
27	CC1317002	6/21/13 18:16	CC1317002_20130621_231658	186	GPS	Cast	
28	CC1317002	6/21/13 18:19	CC1317002_20130621_231929	199	GPS	Cast	Just outside of channel (reached ~7 m depth)
29	CC1317002	6/21/13 18:20	CC1317002_20130621_232024	94	GPS	Point Measurement	

Figure 26: CTD Data Summary for 06/19/2013 Trip

Cast Number	Device	Cast Time (Local)	File Name	Number of Samples	Location Source	Sample Type	Notes
30	CC1317002	7/1/13 18:50	CC1317002_20130701_235040	282	GPS	Invalid	
31	CC1317002	7/1/13 18:52	CC1317002_20130701_235252	409	GPS	Cast	Much deeper than other Mouth W casts
32	CC1317002	7/1/13 19:23	CC1317002_20130702_002358	254	GPS	Cast	Farther offshore than other cast at Mouth E
33	CC1317002	7/1/13 19:51	CC1317002_20130702_005144	662	GPS	Cast	
34	CC1317002	7/1/13 20:06	CC1317002_20130702_010611	672	GPS	Cast	Did not reach channel bottom (reached ~9 m depth)
35	CC1317002	7/1/13 20:09	CC1317002_20130702_010900	848	GPS	Cast	
36	CC1317002	7/1/13 21:55	CC1317002_20130702_025525	384	GPS	Cast	
37	CC1317002	7/1/13 22:25	CC1317002_20130702_032514	347	GPS	Cast	
38	CC1317002	7/1/13 22:36	CC1317002_20130702_033654	473	GPS	Cast	
39	CC1317002	7/1/13 23:43	CC1317002_20130702_044338	227	GPS	Cast	
40	CC1317002	7/2/13 0:06	CC1317002_20130702_050651	187	GPS	Cast	
41	CC1317002	7/2/13 0:41	CC1317002_20130702_054103	336	GPS	Cast	Did not reach channel bottom (reached ~10 m depth)
42	CC1317002	7/2/13 18:23	CC1317002_20130702_232301	234	GPS	Cast	Much closer to shore than other Mouth W casts
43	CC1317002	7/2/13 18:34	CC1317002_20130702_233450	426	GPS	Cast	
44	CC1317002	7/2/13 20:34	CC1317002_20130703_013419	172	GPS	Cast	
45	CC1317002	7/2/13 21:21	CC1317002_20130703_022111	191	GPS	Cast	
46	CC1317002	7/2/13 21:28	CC1317002_20130703_022804	305	GPS	Cast	Just outside of channel (reached ~5 m depth)
47	CC1317002	7/2/13 22:27	CC1317002_20130703_032737	401	GPS	Cast	
48	CC1317002	7/2/13 23:10	CC1317002_20130703_041034	250	GPS	Cast	
49	CC1317002	7/2/13 23:33	CC1317002_20130703_043300	680	GPS	Cast	
50	CC1317002	7/3/13 3:05	CC1317002_20130703_080558	720	GPS	Cast	Only cast at this location
51	CC1317002	7/3/13 3:30	CC1317002_20130703_083034	678	GPS	Cast	
52	CC1317002	7/3/13 8:08	CC1317002_20130703_130834	354	GPS	Cast	
53	CC1317002	7/3/13 8:14	CC1317002_20130703_131429	510	GPS	Cast	Did not reach channel bottom (reached ~13 m depth)
54	CC1317002	7/3/13 9:14	CC1317002_20130703_141432	181	GPS	Cast	
55	CC1317002	7/3/13 9:22	CC1317002_20130703_142242	329	GPS	Cast	
56	CC1317002	7/3/13 9:25	CC1317002_20130703_142538	682	GPS	Cast	

Figure 27: CTD Data Summary for 07/01/2013 Trip

Cast Number	Device	Cast Time (Local)	File Name	Number of Samples	Location Source	Sample Type	Notes
57	CC1317002	7/17/13 18:00	CC1317002_20130717_230028	324	GPS	Cast	
58	CC1317002	7/17/13 18:22	CC1317002_20130717_232205	378	GPS	Cast	
59	CC1317002	7/17/13 18:29	CC1317002_20130717_232949	567	GPS	Cast	
60	CC1317002	7/17/13 20:52	CC1317002_20130718_015240	169	GPS	Cast	
61	CC1317002	7/17/13 21:01	CC1317002_20130718_020104	197	GPS	Cast	
62	CC1317002	7/17/13 21:12	CC1317002_20130718_021213	289	GPS	Cast	
63	CC1317002	7/17/13 21:47	CC1317002_20130718_024743	321	GPS	Cast	
64	CC1317002	7/17/13 21:50	CC1317002_20130718_025041	340	GPS	Cast	
65	CC1317002	7/18/13 2:11	CC1317002_20130718_071112	369	GPS	Cast	
66	CC1317002	7/18/13 2:35	CC1317002_20130718_073537	174	GPS	Cast	
67	CC1317002	7/18/13 2:53	CC1317002_20130718_075328	273	GPS	Cast	
68	CC1317002	7/18/13 3:55	CC1317002_20130718_085529	195	GPS	Cast	
69	CC1317002	7/18/13 4:01	CC1317002_20130718_090113	427	GPS	Cast	
70	CC1317002	7/18/13 18:03	CC1317002_20130718_230355	311	GPS	Cast	
71	CC1317002	7/18/13 19:17	CC1317002_20130719_001705	153	GPS	Cast	
72	CC1317002	7/18/13 19:23	CC1317002_20130719_002331	181	GPS	Cast	
73	CC1317002	7/18/13 19:27	CC1317002_20130719_002727	169	GPS	Cast	
74	CC1317002	7/18/13 19:30	CC1317002_20130719_003041	217	GPS	Cast	
75	CC1317002	7/18/13 19:35	CC1317002_20130719_003524	214	GPS	Cast	
76	CC1317002	7/18/13 19:39	CC1317002_20130719_003913	201	GPS	Cast	
77	CC1317002	7/18/13 19:43	CC1317002_20130719_004308	188	GPS	Cast	
78	CC1317002	7/18/13 19:46	CC1317002_20130719_004656	172	GPS	Cast	
79	CC1317002	7/18/13 19:51	CC1317002_20130719_005108	282	GPS	Cast	
80	CC1317002	7/18/13 19:55	CC1317002_20130719_005504	212	GPS	Cast	
81	CC1317002	7/18/13 19:59	CC1317002_20130719_005917	207	GPS	Cast	
82	CC1317002	7/18/13 20:04	CC1317002_20130719_010405	213	GPS	Cast	
83	CC1317002	7/18/13 20:06	CC1317002_20130719_010643	198	GPS	Cast	
84	CC1317002	7/18/13 20:10	CC1317002_20130719_011033	216	GPS	Cast	
85	CC1317002	7/18/13 20:14	CC1317002_20130719_011447	327	GPS	Cast	
86	CC1317002	7/18/13 20:20	CC1317002_20130719_012000	187	GPS	Cast	
87	CC1317002	7/18/13 20:23	CC1317002_20130719_012359	203	GPS	Cast	
88	CC1317002	7/18/13 20:28	CC1317002_20130719_012852	192	GPS	Cast	
89	CC1317002	7/18/13 20:32	CC1317002_20130719_013252	332	GPS	Cast	
90	CC1317002	7/18/13 20:37	CC1317002_20130719_013703	252	GPS	Cast	
91	CC1317002	7/18/13 20:41	CC1317002_20130719_014114	216	GPS	Cast	
92	CC1317002	7/18/13 20:44	CC1317002_20130719_014457	225	GPS	Cast	
93	CC1317002	7/18/13 20:50	CC1317002_20130719_015028	419	GPS	Cast	
94	CC1317002	7/18/13 20:54	CC1317002_20130719_015431	267	GPS	Cast	
95	CC1317002	7/18/13 21:22	CC1317002_20130719_022218	222	GPS	Cast	
96	CC1317002	7/18/13 21:43	CC1317002_20130719_024329	422	GPS	Cast	
97	CC1317002	7/18/13 21:48	CC1317002_20130719_024856	204	GPS	Cast	
98	CC1317002	7/19/13 1:07	CC1317002_20130719_060743	180	GPS	Cast	
99	CC1317002	7/19/13 1:14	CC1317002_20130719_061415	153	GPS	Cast	
100	CC1317002	7/19/13 1:21	CC1317002_20130719_062106	166	GPS	Cast	
101	CC1317002	7/19/13 1:28	CC1317002_20130719_062823	141	GPS	Cast	
102	CC1317002	7/19/13 1:35	CC1317002_20130719_063549	162	GPS	Cast	
103	CC1317002	7/19/13 1:43	CC1317002_20130719_064303	228	GPS	Cast	
104	CC1317002	7/19/13 1:50	CC1317002_20130719_065001	206	GPS	Cast	
105	CC1317002	7/19/13 1:57	CC1317002_20130719_065746	181	GPS	Cast	
106	CC1317002	7/19/13 2:06	CC1317002_20130719_070600	181	GPS	Cast	
107	CC1317002	7/19/13 2:14	CC1317002_20130719_071408	182	GPS	Cast	
108	CC1317002	7/19/13 2:22	CC1317002_20130719_072235	321	GPS	Cast	
109	CC1317002	7/19/13 2:30	CC1317002_20130719_073056	243	GPS	Cast	
110	CC1317002	7/19/13 2:40	CC1317002_20130719_074011	263	GPS	Cast	
111	CC1317002	7/19/13 2:48	CC1317002_20130719_074815	840	GPS	Cast	

Figure 28: CTD Data Summary for 07/17/2013 Trip

Cast Number	Device	Cast Time (Local)	File Name	Number of Samples	Location Source	Sample Type	Notes
112	CC1317002	8/5/13 22:00	CC1317002_20130806_030022	360	GPS	Cast	
113	CC1317002	8/5/13 22:23	CC1317002_20130806_032311	484	GPS	Cast	
114	CC1317002	8/5/13 22:49	CC1317002_20130806_034943	749	GPS	Cast	
115	CC1317002	8/6/13 0:40	CC1317002_20130806_054010	203	GPS	Cast	
116	CC1317002	8/6/13 1:14	CC1317002_20130806_061458	518	GPS	Cast	
117	CC1317002	8/6/13 1:33	CC1317002_20130806_063333	277	GPS	Cast	
118	CC1317002	8/6/13 1:46	CC1317002_20130806_064643	273	GPS	Cast	
119	CC1317002	8/6/13 5:29	CC1317002_20130806_102904	435	GPS	Cast	
120	CC1317002	8/6/13 5:57	CC1317002_20130806_105706	313	GPS	Cast	
121	CC1317002	8/6/13 6:04	CC1317002_20130806_110439	397	GPS	Cast	
122	CC1317002	8/6/13 7:32	CC1317002_20130806_123215	177	GPS	Cast	
123	CC1317002	8/6/13 8:03	CC1317002_20130806_130345	162	GPS	Cast	
124	CC1317002	8/6/13 8:17	CC1317002_20130806_131747	396	GPS	Cast	
125	CC1317002	8/6/13 8:42	CC1317002_20130807_014258	233	GPS	Cast	

Figure 29: CTD Data Summary for 08/05/2013 Trip

C Data Analysis: Matlab Scripts and Functions

```
close all; clc; clear all;

%%%%%%%%%%%%%%%%%%%%%%%%%%%%%%%%%%%%%%%%%%%%%%%%%%%%%%%%%%%%%%%%%%%%%%%%%%%%
% Title: script_RiverSurveyor_to_ZoneAvgProf
% Author: David Christiansen
% Date Created: 09/06/2013
% Description: This script calls the underlying functions which take
% exported data from RiverSurveyor and convert it into a structure called
% zones.  This structure includes spatially averaged velocity profiles for
% each of the three zones in the along- and cross-channel directions, as
% well as the corresponding std dev profiles.  Also included are the raw
% profiles organized by zone.
%%%%%%%%%%%%%%%%%%%%%%%%%%%%%%%%%%%%%%%%%%%%%%%%%%%%%%%%%%%%%%%%%%%%%%%%%%%%

fnamelist = {'20130806003705'...
             '20130806005105',...
             '20130806005710',...
             '20130806012407',...
             '20130806014109',...
             '20130806073730',...
             '20130806080609'...
             };

coarsegrid = 1;
for kk=1:length(fnamelist)
        data = fnamelist{kk};
        function_RiverSurveyor_to_convert_ENU(data)
        [depthvector] = function_Fluxes_ChanDirtransects(data,coarsegrid);
        function_Avg_VelProf(data)
end
```

```
%%%%%%%%%%%%%%%%%%%%%%%%%%%%%%%%%%%%%%%%%%%%%%%%%%%%%%%%%%%%%%%%%%%%%%%%%%%%
% Title: function_RiverSurveyor_to_convert_ENU
% Author: David Christiansen
% Date Created: 09/06/2013
% Description: This code was developed to convert exported data from
% RiverSurveyor into one structure containing all valuable data for one
% RiverSurveyor file.
%%%%%%%%%%%%%%%%%%%%%%%%%%%%%%%%%%%%%%%%%%%%%%%%%%%%%%%%%%%%%%%%%%%%%%%%%%%%

function [] = function_RiverSurveyor_to_convert_ENU(filename)


% load('/Users/dachrist/Dropbox/HydroSurveyor_Projects/HSgalveston/...
...galvestonbay_08052013/2013_08_07/20130805213304.mat')
load(['/Users/davechristinason/Dropbox/HydroSurveyor_Projects'...
'/HSgalveston/galvestonbay_08052013/' filename '.mat'])

WaterVelE = zeros(size(WaterTrack.Velocity,1),size(WaterTrack.Velocity,3));
WaterVelN = zeros(size(WaterTrack.Velocity,1),size(WaterTrack.Velocity,3));
WaterVelU = zeros(size(WaterTrack.Velocity,1),size(WaterTrack.Velocity,3));
WaterVelD = zeros(size(WaterTrack.Velocity,1),size(WaterTrack.Velocity,3));

for ii = 1:size(WaterVelE,1)
    for jj = 1:size(WaterVelE,2)
        WaterVelE(ii,jj) = WaterTrack.Velocity(ii,1,jj);
        WaterVelN(ii,jj) = WaterTrack.Velocity(ii,2,jj);
        WaterVelU(ii,jj) = WaterTrack.Velocity(ii,3,jj);
        WaterVelD(ii,jj) = WaterTrack.Velocity(ii,4,jj);
    end
end
clear ii; clear jj;
display('thru first loop')

WaterVelEnew = zeros(size(WaterVelE,2),size(WaterVelE,1));
WaterVelNnew = zeros(size(WaterVelE,2),size(WaterVelE,1));
WaterVelUnew = zeros(size(WaterVelE,2),size(WaterVelE,1));
WaterVelDnew = zeros(size(WaterVelE,2),size(WaterVelE,1));

WaterVelEnew = WaterVelE';
WaterVelNnew = WaterVelN';
WaterVelUnew = WaterVelU';
WaterVelDnew = WaterVelD';

WaterVelCube = zeros(size(WaterVelEnew,1),size(WaterVelEnew,2),4);
```

```
WaterVelCube(:,:,1) = WaterVelEnew;
WaterVelCube(:,:,2) = WaterVelNnew;
WaterVelCube(:,:,3) = WaterVelUnew;
WaterVelCube(:,:,4) = WaterVelDnew;

MaxADCPDepth = max(BottomTrack.BT_Depth);
MinCellSize = min(System.Cell_Size);
num_div = zeros(size(WaterVelCube,1));
num_div_start = zeros(size(WaterVelCube,1));

for jj=1:size(WaterVelCube,1)
    num_div(jj)=round(System.Cell_Size(jj)/ MinCellSize);
    num_div_start(jj)= round(System.Cell_Start(jj)/ MinCellSize);
end
clear jj;
display('thru second loop')

north_vel = zeros(size(WaterVelCube,1),MaxADCPDepth/MinCellSize);
east_vel = zeros(size(WaterVelCube,1),MaxADCPDepth/MinCellSize);
up_vel = zeros(size(WaterVelCube,1),MaxADCPDepth/MinCellSize);
err_vel = zeros(size(WaterVelCube,1),MaxADCPDepth/MinCellSize);


for ii = 1:size(WaterVelCube,1)
    count = 1;
    for jj = num_div(ii):num_div(ii):size(north_vel,2)
        if count <= size(WaterVelCube,2)
            north_vel(ii,(jj - (num_div(ii) - 1):jj)) = ...
                WaterVelCube(ii,count,2);
            east_vel(ii,jj - (num_div(ii) - 1):jj) = ...
                WaterVelCube(ii,count,1);
            up_vel(ii,jj - (num_div(ii) - 1):jj) = ...
                WaterVelCube(ii,count,3);
            err_vel(ii,jj - (num_div(ii) - 1):jj) = ...
                WaterVelCube(ii,count,4);
            count = count + 1;
        else
        end
    end
end

% north_vel = WaterVelCube(:,:,2)';
% east_vel = WaterVelCube(:,:,1)';
% up_vel = WaterVelCube(:,:,3)';
% err_vel = WaterVelCube(:,:,4)';
```

```
clear ii; clear jj;
display('thru third loop')

for ii = 1:size(north_vel,1)
    for jj = 1:size(north_vel,2)
        if jj * MinCellSize <= BottomTrack.BT_Depth(ii)
        else
            north_vel(ii,jj) = NaN;
            east_vel(ii,jj) = NaN;
            up_vel(ii,jj) = NaN;
            err_vel(ii,jj) = NaN;
        end
    end
end
display('thru fourth loop')

clear ii; clear jj;
display('saving')

structname = ['Session' filename];

STRUCT.(structname).WVENUCube = WaterVelCube;
% Session20130719_073313.BTBeam1OffsetEastm = BTBeam1OffsetEastm;
% Session20130719_073313.BTBeam1OffsetNorthm = BTBeam1OffsetNorthm;
STRUCT.(structname).BTBeam1Rangem = BottomTrack.BT_Beam_Depth(:,1);
% Session20130719_073313.BTBeam2OffsetEastm = BTBeam2OffsetEastm;
% Session20130719_073313.BTBeam2OffsetNorthm = BTBeam2OffsetNorthm;
STRUCT.(structname).BTBeam2Rangem = BottomTrack.BT_Beam_Depth(:,2);
% Session20130719_073313.BTBeam3OffsetEastm = BTBeam3OffsetEastm;
% Session20130719_073313.BTBeam3OffsetNorthm = BTBeam3OffsetNorthm;
STRUCT.(structname).BTBeam3Rangem = BottomTrack.BT_Beam_Depth(:,3);
% Session20130719_073313.BTBeam4OffsetEastm = BTBeam4OffsetEastm;
% Session20130719_073313.BTBeam4OffsetNorthm = BTBeam4OffsetNorthm;
STRUCT.(structname).BTBeam4Rangem = BottomTrack.BT_Beam_Depth(:,4);
STRUCT.(structname).BTVelDms = BottomTrack.BT_Vel(:,4);
STRUCT.(structname).BTVelEms = BottomTrack.BT_Vel(:,1);
STRUCT.(structname).BTVelNms = BottomTrack.BT_Vel(:,2);
STRUCT.(structname).BTVelUms = BottomTrack.BT_Vel(:,3);
STRUCT.(structname).BTrange_avg = BottomTrack.BT_Depth;
STRUCT.(structname).CellSizem = System.Cell_Size;
STRUCT.(structname).CellStartm = System.Cell_Start;
STRUCT.(structname).DateTime = datestr((System.Time) ./ (3600*24)+1);
STRUCT.(structname).FrequencyMHz = WaterTrack.WT_Frequency;
STRUCT.(structname).Headingrad = System.Heading;
```

```
STRUCT.(structname).Latitudedeg = GPS.Latitude;
STRUCT.(structname).Longitudedeg = GPS.Longitude;
STRUCT.(structname).Pitchrad = System.Pitch;
STRUCT.(structname).Rollrad = System.Roll;
% Session20130719_073313.SampleNumber = SampleNumber;
STRUCT.(structname).UTMEastingm = GPS.UTM(:,1);
STRUCT.(structname).UTMNorthingm = GPS.UTM(:,2);
% Session20130719_073313.UTMZoneLetter = UTMZoneLetter;
% Session20130719_073313.UTMZoneNumber = UTMZoneNumber;
STRUCT.(structname).VBDepthm = BottomTrack.VB_Depth;
STRUCT.(structname).WaterVelD = WaterTrack.Velocity(:,4,:);
STRUCT.(structname).WaterVelE = WaterTrack.Velocity(:,1,:);
STRUCT.(structname).WaterVelN = WaterTrack.Velocity(:,2,:);
STRUCT.(structname).WaterVelU = WaterTrack.Velocity(:,3,:);
STRUCT.(structname).north_vel = north_vel';
STRUCT.(structname).east_vel = east_vel';
STRUCT.(structname).up_vel = up_vel';
STRUCT.(structname).err_vel = err_vel';
STRUCT.(structname).MinCellSize = MinCellSize;
if STRUCT.(structname).Latitudedeg(1) > 29.45
    STRUCT.(structname).chandir = 147;
elseif STRUCT.(structname).Latitudedeg(1) < 29.45
    STRUCT.(structname).chandir = 138;
end

ADCPData = STRUCT.(structname);

% save('/Users/dachrist/Dropbox/HydroSurveyor_Projects/HSgalveston/...
...galvestonbay_08052013/2013_08_07/Session20130805213304','...
    ...Session20130805213304');
save(['/Users/davechristinason/Dropbox/HydroSurveyor_Projects/'...
'HSgalveston/galvestonbay_08052013/2013_08_07/' filename ...
'_ADCPData'],'ADCPData')
end
```

```
%%%%%%%%%%%%%%%%%%%%%%%%%%%%%%%%%%%%%%%%%%%%%%%%%%%%%%%%%%%%%%%%%%%%%%%%%%%
% Title: function_Fluxes_ChanDirtransects
% Author: David Christiansen
% Date Created: 07/30/2013
% Description:  This function converts the data from ENU coords to along-
% and cross-channel components.  It plots the along-channel vels, and asks
% the user to input how many zones they wish to break the data up into.
% Once the user enters a number, they are then prompted to selected the
% dividing points between each zone.  This function then saves the data
% broken up into each zone as specified by the user.
%%%%%%%%%%%%%%%%%%%%%%%%%%%%%%%%%%%%%%%%%%%%%%%%%%%%%%%%%%%%%%%%%%%%%%%%%%%

function[depthvector] = ...
    function_Fluxes_ChanDirtransects(filename, coarsegrid);

load(['/Users/davechristinason/Dropbox/HydroSurveyor_Projects'...
    '/HSgalveston/galvestonbay_08052013/2013_08_07/' filename...
    '_ADCPData.mat'])

chandir = ADCPData.chandir;

%% Creating a vector of the depths of measurements for plotting purposes
%%later.
ymax = size(ADCPData.north_vel,1) * ADCPData.MinCellSize;

zone.depthvector = ADCPData.MinCellSize:ADCPData.MinCellSize:ymax;

clear ii;clear jj;

for ii = 1:size(ADCPData.north_vel,1)
    for jj = 1:size(ADCPData.east_vel,2)
        ADCPData.magvel(ii,jj) = sqrt(ADCPData.east_vel(ii,jj) ^ 2 + ...
            ADCPData.north_vel(ii,jj) ^ 2);
        if isnan(ADCPData.north_vel(ii,jj)) == 1
            ADCPData.dirvel(ii,jj) = NaN;
        elseif ADCPData.north_vel(ii,jj) == 0
            if ADCPData.east_vel(ii,jj) > 0
                ADCPData.dirvel(ii,jj) = 90;
            elseif ADCPData.east_vel(ii,jj) < 0
                ADCPData.dirvel(ii,jj) = 270;
            else
                ADCPData.dirvel(ii,jj) = NaN;
            end
        elseif ADCPData.north_vel(ii,jj) > 0
            if ADCPData.east_vel(ii,jj) > 0
```

```
                ADCPData.dirvel(ii,jj) = atand(ADCPData.east_vel(ii,jj)...
                    /ADCPData.north_vel(ii,jj));
            elseif ADCPData.east_vel(ii,jj) == 0
                ADCPData.dirvel(ii,jj) = 360;
            else
                ADCPData.dirvel(ii,jj) = atand(ADCPData.east_vel(ii,jj)...
                    /ADCPData.north_vel(ii,jj)) + 360;
            end
        elseif ADCPData.north_vel(ii,jj) < 0
            if ADCPData.east_vel(ii,jj) == 0
                ADCPData.dirvel(ii,jj) = 180;
            else
                ADCPData.dirvel(ii,jj) = atand(ADCPData.east_vel(ii,jj)...
                    /ADCPData.north_vel(ii,jj)) + 180;
            end
        end
    end
end
clear ii; clear jj;

for ii = 1:size(ADCPData.north_vel,1)
    for jj = 1:size(ADCPData.east_vel,2)
        if ADCPData.dirvel(ii,jj) == chandir - 90
            ADCPData.along_vel(ii,jj) = 0;
            ADCPData.cross_vel(ii,jj) = ADCPData.magvel(ii,jj);
%             display('cross axis +')
        elseif isnan(ADCPData.dirvel(ii,jj)) == 1
            ADCPData.along_vel(ii,jj) = NaN;
            ADCPData.cross_vel(ii,jj) = NaN;
%             display('NaN')
        elseif ADCPData.dirvel(ii,jj) > chandir - 90
            if ADCPData.dirvel(ii,jj) < chandir
                ADCPData.along_vel(ii,jj) = ADCPData.magvel(ii,jj) *...
                    cosd(chandir - ADCPData.dirvel(ii,jj));
                ADCPData.cross_vel(ii,jj) = ADCPData.magvel(ii,jj) *...
                    sind(chandir - ADCPData.dirvel(ii,jj));
%                 display('1st Quad')
            elseif ADCPData.dirvel(ii,jj) == chandir
                ADCPData.along_vel(ii,jj) = ADCPData.magvel(ii,jj);
                ADCPData.cross_vel(ii,jj) = 0;
%                 display('along axis +')
            elseif ADCPData.dirvel(ii,jj) < chandir +90
                ADCPData.along_vel(ii,jj) = ADCPData.magvel(ii,jj) *...
                    cosd(chandir - ADCPData.dirvel(ii,jj));
                ADCPData.cross_vel(ii,jj) = ADCPData.magvel(ii,jj) *...
```

```
                    sind(chandir - ADCPData.dirvel(ii,jj));
%                   display('2nd Quad')
            elseif ADCPData.dirvel(ii,jj) == chandir + 90
                ADCPData.along_vel(ii,jj) = 0;
                ADCPData.cross_vel(ii,jj) = (-1) * ADCPData.magvel(ii,jj);
%                   display('cross axis -')
            elseif ADCPData.dirvel(ii,jj) < chandir +180
                ADCPData.along_vel(ii,jj) = ADCPData.magvel(ii,jj) *...
                    sind(chandir + 90 - ADCPData.dirvel(ii,jj));
                ADCPData.cross_vel(ii,jj) = (-1) *...
                    ADCPData.magvel(ii,jj) * cosd(chandir + 90 - ...
                    ADCPData.dirvel(ii,jj));
%                   display('3rd Quad')
            elseif ADCPData.dirvel(ii,jj) == chandir + 180
                ADCPData.along_vel(ii,jj) = (-1) * ADCPData.magvel(ii,jj);
                ADCPData.cross_vel(ii,jj) = 0;
%                   display('along axis -')
            elseif ADCPData.dirvel(ii,jj) < chandir + 270
                ADCPData.along_vel(ii,jj) = (-1) *...
                    ADCPData.magvel(ii,jj) * cosd(chandir +...
                    180 - ADCPData.dirvel(ii,jj));
                ADCPData.cross_vel(ii,jj) = (-1) *...
                    ADCPData.magvel(ii,jj) * sind(chandir +...
                    180 - ADCPData.dirvel(ii,jj));
%                   display('4th Quad')
            end
        end
    end
end

clear ii; clear jj;

% ADCPData.along_vel = ADCPData.magvel .* cos(chandir - ADCPData.dirvel);
% ADCPData.cross_vel = ADCPData.magvel .* sin(chandir - ADCPData.dirvel);

%% Creating course grid ADCPData matrices by averaging 'coarsegrid'
%%ADCPDatas together in both the x and y directions.
CGtransAlongAvg = zeros(size(ADCPData.east_vel));
CGtransCrossAvg = zeros(size(ADCPData.east_vel));
CGtransUAvg = zeros(size(ADCPData.east_vel));

for ii = coarsegrid:coarsegrid:size(ADCPData.east_vel,1)
    for jj = coarsegrid:coarsegrid:size(ADCPData.east_vel,2)
        CGtransAlongAvg(ii - (coarsegrid - 1):ii,(jj -...
            (coarsegrid - 1)):jj) = nanmean(nanmean(ADCPData.along_vel...
```

```
            (ii-(coarsegrid-1):ii,(jj - (coarsegrid - 1)):jj)));
        CGtransCrossAvg(ii - (coarsegrid - 1):ii,(jj -...
            (coarsegrid - 1)):jj) = nanmean(nanmean(ADCPData.cross_vel...
            (ii-(coarsegrid-1):ii,(jj - (coarsegrid - 1)):jj)));
        CGtransUAvg(ii - (coarsegrid - 1):ii,(jj - (coarsegrid - 1)):jj)...
            = nanmean(nanmean(ADCPData.up_vel(ii-(coarsegrid-1):ii,(jj...
            - (coarsegrid - 1)):jj)));
    end
end

clear ii;clear jj;

%% A repeat of earlier section to remove any erronous data below the
%%average bottom depth.

for ii = 1:size(ADCPData.north_vel,2)
    for jj = 1:size(ADCPData.north_vel,1)
        if jj * ADCPData.MinCellSize <= ADCPData.BTrange_avg(ii)
        else
            CGtransAlongAvg(jj,ii) = NaN;
            CGtransCrossAvg(jj,ii) = NaN;
            CGtransUAvg(jj,ii) = NaN;
        end
    end
end

clear ii; clear jj;
%% Plotting coarse grid of easting, northing, and upwards velocities
figure;
imagesc(1:size(ADCPData.east_vel,2),zone.depthvector,CGtransAlongAvg)
set(gca,'xticklabel',{[]})
% set(gca, 'XTick', size(ADCPData.east_vel,2)/10:size...
...(ADCPData.east_vel,2)/5:size(ADCPData.east_vel,2), 'XTickLabel',...
...ADCPData.datetime(1:size(ADCPData.east_vel,2)/5:size...
...(ADCPData.east_vel,2)));
title('ADCP Across-Channel Vel (m/s)','fontsize',28,'fontweight','bold')
ylabel('Depth (m)','fontsize',28,'fontweight','bold')
ylim([0 20])
colorbar
caxis([-1.5 1.5])
set(gca,'FontSize',26,'FontWeight','bold')
gg = colormap(gcf);
gg(1,:) = 0.5;
colormap(gg)
axis ij
```

```
zone.userinput = input('How many zones? \n');

zone.zonex(1) = 1;

[zone.zonex(2:zone.userinput),zoney] = ginput(zone.userinput - 1);

zone.zonex(zone.userinput + 1) = size(CGtransAlongAvg,2);

clear jj;

zone.FluxAlong.Flux = zeros(zone.userinput);
zone.FluxCross.Flux = zeros(zone.userinput);
zone.FluxU.Flux = zeros(zone.userinput);
zone.FluxAlong.varvectors = zeros(5,607980);
zone.FluxAlong.varvectors = zeros(5,607980);
zone.FluxAlong.varvectors = zeros(5,607980);
zone.FluxAlong.numbins = zeros(zone.userinput);
zone.FluxCross.numbins = zeros(zone.userinput);
zone.FluxU.numbins = zeros(zone.userinput);

clear ii;
for ii = 1:zone.userinput
    zone.DepthAvg(ii) =...
        nanmean(ADCPData.BTrange_avg(zone.zonex(ii):zone.zonex(ii+1)));
    zone.FluxAlong.Flux(ii) =...
        nansum(nansum(ADCPData.along_vel(:,zone.zonex(ii):...
        zone.zonex(ii+1))));
    zone.FluxCross.Flux(ii) =...
        nansum(nansum(ADCPData.cross_vel(:,zone.zonex(ii):...
        zone.zonex(ii+1))));
    zone.FluxU.Flux(ii) =...
        nansum(nansum(ADCPData.up_vel(:,zone.zonex(ii):zone.zonex(ii+1))));
    count = 0;
    for jj = 1:floor(size(ADCPData.along_vel,1))
        zone.FluxAlong.varvectors(ii,count+1:count +...
            (zone.zonex(ii+1) - zone.zonex(ii)) + 1) =...
            (ADCPData.along_vel(jj,zone.zonex(ii):zone.zonex(ii+1)));
        zone.FluxCross.varvectors(ii,count+1:count +...
            (zone.zonex(ii+1) - zone.zonex(ii)) + 1) =...
            (ADCPData.cross_vel(jj,zone.zonex(ii):zone.zonex(ii+1)));
        zone.FluxU.varvectors(ii,count+1:count +...
            (zone.zonex(ii+1) - zone.zonex(ii)) + 1) =...
            (ADCPData.up_vel(jj,zone.zonex(ii):zone.zonex(ii+1)));
        count = count + (zone.zonex(ii+1) - zone.zonex(ii)) + 1;
```

```
    end
    zone.FluxAlong.numbins(ii) = size(zone.FluxAlong.varvectors(ii,:),2)...
        - nansum(nansum(isnan(zone.FluxAlong.varvectors(ii,:))));
    zone.FluxCross.numbins(ii) = size(zone.FluxCross.varvectors(ii,:),2)...
        - nansum(nansum(isnan(zone.FluxCross.varvectors(ii,:))));
    zone.FluxU.numbins(ii) = size(zone.FluxU.varvectors(ii,:),2) -...
        nansum(nansum(isnan(zone.FluxU.varvectors(ii,:))));
end

zone.FluxAlong.Var = zeros(zone.userinput);
zone.FluxCross.Var = zeros(zone.userinput);
zone.FluxU.Var = zeros(zone.userinput);
zone.FluxAlong.Var = nanvar(zone.FluxAlong.varvectors,2);
zone.FluxCross.Var = nanvar(zone.FluxCross.varvectors,2);
zone.FluxU.Var = nanvar(zone.FluxU.varvectors,2);

% for ii = 1:size(ADCPData.along_vel,1)
%     for jj = 1:size(ADCPData.along_vel,2)
%         zone.FluxAlong.Var(ii,jj) =...
...(ADCPData.along_vel(:,zone.zonex(ii):zone.zonex(ii+1));
%         zone.FluxCross.Var(ii,jj) =...
...nanvar(ADCPData.cross_vel(:,zone.zonex(ii):zone.zonex(ii+1)));
%         zone.FluxU.Var(ii,jj) =...
...nanvar(ADCPData.up_vel(:,zone.zonex(ii):zone.zonex(ii+1)));

clear ii;clear jj;

zone.FluxAlong.FluxTrans = zeros(size(ADCPData.along_vel));
zone.FluxCross.FluxTrans = zeros(size(ADCPData.cross_vel));
zone.FluxU.FluxTrans = zeros(size(ADCPData.up_vel));
zone.FluxAlong.VelProf = zeros(size(ADCPData.along_vel,1),zone.userinput);
zone.FluxCross.VelProf = zeros(size(ADCPData.cross_vel,1),zone.userinput);
zone.FluxU.VelProf = zeros(size(ADCPData.up_vel,1),zone.userinput);
zone.FluxAlong.ErrProf = zeros(size(ADCPData.along_vel,1),zone.userinput);
zone.FluxCross.ErrProf = zeros(size(ADCPData.cross_vel,1),zone.userinput);
zone.FluxU.ErrProf = zeros(size(ADCPData.up_vel,1),zone.userinput);

for ii = 1:zone.userinput
    for jj = 1:floor(size(ADCPData.along_vel,1))
        zone.FluxAlong.FluxTrans(jj,zone.zonex(ii):zone.zonex(ii+1)) =...
            nansum(nansum(ADCPData.along_vel(:,zone.zonex(ii):...
            zone.zonex(ii+1))));
        zone.FluxCross.FluxTrans(jj,zone.zonex(ii):zone.zonex(ii+1)) =...
            nansum(nansum(ADCPData.cross_vel(:,zone.zonex(ii):...
            zone.zonex(ii+1))));
```

```
        zone.FluxU.FluxTrans(jj,zone.zonex(ii):zone.zonex(ii+1)) =...
            nansum(nansum(ADCPData.up_vel(:,zone.zonex(ii):...
            zone.zonex(ii+1))));
        zone.FluxAlong.VelProf(jj,ii) =...
            nanmean(ADCPData.along_vel(jj,zone.zonex(ii):...
            zone.zonex(ii+1)),2);
        zone.FluxCross.VelProf(jj,ii) =...
            nanmean(ADCPData.cross_vel(jj,zone.zonex(ii):...
            zone.zonex(ii+1)),2);
        zone.FluxU.VelProf(jj,ii) =...
            nanmean(ADCPData.up_vel(jj,zone.zonex(ii):...
            zone.zonex(ii+1)),2);
        zone.FluxAlong.ErrProf(jj,ii) =...
            nanvar(ADCPData.along_vel(jj,zone.zonex(ii):...
            zone.zonex(ii+1)));
        zone.FluxCross.ErrProf(jj,ii) =...
            nanvar(ADCPData.cross_vel(jj,zone.zonex(ii):...
            zone.zonex(ii+1)));
        zone.FluxU.ErrProf(jj,ii) =...
            nanvar(ADCPData.up_vel(jj,zone.zonex(ii):...
            zone.zonex(ii+1)));
    end
end
clear ii; clear jj;

for ii = 1:size(ADCPData.north_vel,2)
    for jj = 1:size(ADCPData.north_vel,1)
        if jj * ADCPData.MinCellSize <= ADCPData.BTrange_avg(ii)
        else
            zone.FluxAlong.FluxTrans(jj,ii) = NaN;
            zone.FluxCross.FluxTrans(jj,ii) = NaN;
            zone.FluxU.FluxTrans(jj,ii) = NaN;
        end
    end
end

save(['/Users/davechristinason/Dropbox/HydroSurveyor_Projects'...
    '/HSgalveston/galvestonbay_08052013/2013_08_07/' filename...
    '_fluxes.mat'],'zone')
depthvector = zone.depthvector;
end
```

```
%%%%%%%%%%%%%%%%%%%%%%%%%%%%%%%%%%%%%%%%%%%%%%%%%%%%%%%%%%%%%%%%%%%%%%%%%%%
% Title: function_Avg_VelProf
% Author: David Christiansen
% Date Created: 09/06/2013
% Description: This code uses structures created by
% function_Fluxes_ChanDirtransects and
% function_RiverSurveyor_to_convert_ENU.  It shows the data broken up
% earlier and asks what if the zones specified are zone 1, 2, or 3.  User
% must select 1, 2, or 3 and press enter.  The user must continue entering
% zone numbers until all divisions of the data have been assigned a zone
% number.  This function then appends the "zone" structure to include
% spatially averaged along- and cross-channel velocity profiles for each
% zone, as well as corresponding std dev profiles.  It also includes the
% raw profiles for each zone.
%%%%%%%%%%%%%%%%%%%%%%%%%%%%%%%%%%%%%%%%%%%%%%%%%%%%%%%%%%%%%%%%%%%%%%%%%%%

function [] = function_Avg_VelProf(filename)

load(['/Users/davechristinason/Dropbox/HydroSurveyor_Projects/'...
    'HSgalveston/galvestonbay_08052013/2013_08_07/' filename ...
    '_fluxes.mat'])
load(['/Users/davechristinason/Dropbox/HydroSurveyor_Projects/'...
    'HSgalveston/galvestonbay_08052013/2013_08_07/' filename ...
    '_ADCPData.mat'])

figure;
title(filename);
imagesc(1:size(ADCPData.east_vel,2),zone.depthvector,ADCPData.east_vel)
set(gca,'xticklabel',{[]})
% set(gca, 'XTick', size(ADCPData.east_vel,2)/10:...
...size(ADCPData.east_vel,2)/5:size(ADCPData.east_vel,2),...
...'XTickLabel', ADCPData.datetime(1:size(ADCPData.east_vel,2)/5:size...
...(ADCPData.east_vel,2)));
% title('ADCP Along-Channel Vel (m/s)','fontsize',28,'fontweight','bold')
ylabel('Depth (m)','fontsize',28,'fontweight','bold')
ylim([0 20])
colorbar
caxis([-1.5 1.5])
set(gca,'FontSize',26,'FontWeight','bold')
gg = colormap(gcf);
gg(1,:) = 0.5;
colormap(gg)
axis ij

zone.order = zeros(size(zone.FluxAlong.VelProf,2),1);
```

```
for ii = 1:length(zone.order)
    zone.order(ii) = ...
        input('Order of zones? (1 = SW end, 2 = HSC, 3 = NE end) \n');
end
clear ii;

ones = zeros(size(zone.order));
twos = zeros(size(zone.order));
threes = zeros(size(zone.order));

ones = find(zone.order == 1);
twos = find(zone.order == 2);
threes = find(zone.order == 3);

zone.DepthAvg1 = nanmean(zone.DepthAvg(ones));
zone.DepthAvg2 = nanmean(zone.DepthAvg(twos));
zone.DepthAvg3 = nanmean(zone.DepthAvg(threes));

zone.FluxAlong.avg1 = zeros(size(zone.FluxAlong.VelProf,1));
zone.FluxAlong.avg2 = zeros(size(zone.FluxAlong.VelProf,1));
zone.FluxAlong.avg3 = zeros(size(zone.FluxAlong.VelProf,1));
zone.FluxCross.avg1 = zeros(size(zone.FluxAlong.VelProf,1));
zone.FluxCross.avg2 = zeros(size(zone.FluxAlong.VelProf,1));
zone.FluxCross.avg3 = zeros(size(zone.FluxAlong.VelProf,1));
zone.FluxU.avg1 = zeros(size(zone.FluxAlong.VelProf,1));
zone.FluxU.avg2 = zeros(size(zone.FluxAlong.VelProf,1));
zone.FluxU.avg3 = zeros(size(zone.FluxAlong.VelProf,1));
zone.FluxAlong.avg1err = zeros(size(zone.FluxAlong.VelProf,1));
zone.FluxAlong.avg2err = zeros(size(zone.FluxAlong.VelProf,1));
zone.FluxAlong.avg3err = zeros(size(zone.FluxAlong.VelProf,1));
zone.FluxCross.avg1err = zeros(size(zone.FluxAlong.VelProf,1));
zone.FluxCross.avg2err = zeros(size(zone.FluxAlong.VelProf,1));
zone.FluxCross.avg3err = zeros(size(zone.FluxAlong.VelProf,1));
zone.FluxU.avg1err = zeros(size(zone.FluxAlong.VelProf,1));
zone.FluxU.avg2err = zeros(size(zone.FluxAlong.VelProf,1));
zone.FluxU.avg3err = zeros(size(zone.FluxAlong.VelProf,1));

zone.FluxAlong.avg1 = nanmean(zone.FluxAlong.VelProf(:,ones),2);
zone.FluxCross.avg1 = nanmean(zone.FluxCross.VelProf(:,ones),2);
zone.FluxU.avg1 = nanmean(zone.FluxU.VelProf(:,ones),2);
zone.FluxAlong.avg2 = nanmean(zone.FluxAlong.VelProf(:,twos),2);
zone.FluxCross.avg2 = nanmean(zone.FluxCross.VelProf(:,twos),2);
zone.FluxU.avg2 = nanmean(zone.FluxU.VelProf(:,twos),2);
zone.FluxAlong.avg3 = nanmean(zone.FluxAlong.VelProf(:,threes),2);
```

```
zone.FluxCross.avg3 = nanmean(zone.FluxCross.VelProf(:,threes),2);
zone.FluxU.avg3 = nanmean(zone.FluxU.VelProf(:,threes),2);
zone.FluxAlong.avg1err = nanmean(zone.FluxAlong.ErrProf(:,ones),2);
zone.FluxCross.avg1err = nanmean(zone.FluxCross.ErrProf(:,ones),2);
zone.FluxU.avg1err = nanmean(zone.FluxU.ErrProf(:,ones),2);
zone.FluxAlong.avg2err = nanmean(zone.FluxAlong.ErrProf(:,twos),2);
zone.FluxCross.avg2err = nanmean(zone.FluxCross.ErrProf(:,twos),2);
zone.FluxU.avg2err = nanmean(zone.FluxU.ErrProf(:,twos),2);
zone.FluxAlong.avg3err = nanmean(zone.FluxAlong.ErrProf(:,threes),2);
zone.FluxCross.avg3err = nanmean(zone.FluxCross.ErrProf(:,threes),2);
zone.FluxU.avg3err = nanmean(zone.FluxU.ErrProf(:,threes),2);
zone.FluxAlong.avg1std = nanstd(zone.FluxAlong.VelProf(:,ones),2);
zone.FluxCross.avg1std = nanstd(zone.FluxCross.VelProf(:,ones),2);
zone.FluxU.avg1std = nanstd(zone.FluxU.VelProf(:,ones),2);
zone.FluxAlong.avg2std = nanstd(zone.FluxAlong.VelProf(:,twos),2);
zone.FluxCross.avg2std = nanstd(zone.FluxCross.VelProf(:,twos),2);
zone.FluxU.avg2std = nanstd(zone.FluxU.VelProf(:,twos),2);
zone.FluxAlong.avg3std = nanstd(zone.FluxAlong.VelProf(:,threes),2);
zone.FluxCross.avg3std = nanstd(zone.FluxCross.VelProf(:,threes),2);
zone.FluxU.avg3std = nanstd(zone.FluxU.VelProf(:,threes),2);

zone.FluxAlong.ones = zone.FluxAlong.VelProf(:,ones);
zone.FluxCross.ones = zone.FluxCross.VelProf(:,ones);
% zone.FluxU.avg1 = nanmean(zone.FluxU.VelProf(:,ones),2);
zone.FluxAlong.twos = zone.FluxAlong.VelProf(:,twos);
zone.FluxCross.twos = zone.FluxCross.VelProf(:,twos);
% zone.FluxU.avg2 = nanmean(zone.FluxU.VelProf(:,twos),2);
zone.FluxAlong.threes = zone.FluxAlong.VelProf(:,threes);
zone.FluxCross.threes = zone.FluxCross.VelProf(:,threes);
% zone.FluxU.avg3 = nanmean(zone.FluxU.VelProf(:,threes),2);
% zone.FluxAlong.avg1err = nanmean(zone.FluxAlong.ErrProf(:,ones),2);
% zone.FluxCross.avg1err = nanmean(zone.FluxCross.ErrProf(:,ones),2);
% zone.FluxU.avg1err = nanmean(zone.FluxU.ErrProf(:,ones),2);
% zone.FluxAlong.avg2err = nanmean(zone.FluxAlong.ErrProf(:,twos),2);
% zone.FluxCross.avg2err = nanmean(zone.FluxCross.ErrProf(:,twos),2);
% zone.FluxU.avg2err = nanmean(zone.FluxU.ErrProf(:,twos),2);
% zone.FluxAlong.avg3err = nanmean(zone.FluxAlong.ErrProf(:,threes),2);
% zone.FluxCross.avg3err = nanmean(zone.FluxCross.ErrProf(:,threes),2);
% zone.FluxU.avg3err = nanmean(zone.FluxU.ErrProf(:,threes),2);

save(['/Users/dachrist/Dropbox/HydroSurveyor_Projects/'...
    'HSgalveston/galvestonbay_08052013/2013_08_07/' filename ...
    '_fluxes.mat'],'zone')

end
```

References

Barth, J. A. and K. H. Brink (1987). Shipboard acoustic Doppler profiler velocity observations near Point Conception - spring 1983. *Journal of Geophysical Research-Oceans 92*(C4), 3925–3943.

Brierley, A. S., M. A. Brandon, and J. L. Watkins (1998). An assessment of the utility of an acoustic Doppler current profiler for biomass estimation. *Deep-Sea Research Part I-Oceanographic Research Papers 45*(9), 1555–1573.

Buijsman, M. C. and H. Ridderinkhof (2007). Long-term ferry-ADCP observations of tidal currents in the Marsdiep Inlet. *Journal of Sea Research 57*(4), 237–256.

Callede, J., P. Kosuth, J. L. Guyot, and V. S. Guimaraes (2000). Discharge determination by acoustic Doppler current profilers (ADCP): a moving bottom error correction method and its application on the River Amazon at Obidos. *Hydrological Sciences Journal-Journal Des Sciences Hydrologiques 45*(6), 911–924.

Casebeer, D. (2013, November). Phone interview.

Chant, R. J., W. R. Geyer, R. Houghton, E. Hunter, and J. Lerczak (2007). Estuarine boundary layer mixing processes: Insights from dye experiments. *Journal of Physical Oceanography 37*(7), 1859–1877.

Chant, R. J. and R. E. Wilson (1997). Secondary circulation in a highly stratified estuary. *Journal of Geophysical Research-Oceans 102*(C10), 23207–23215.

Chant, R. J. and R. E. Wilson (2000). Internal hydraulics and mixing in a highly stratified estuary. *Journal of Geophysical Research-Oceans 105*(C6), 14215–14222.

Chapman, P. (2013). Gulf Integrated Spill Research Consortium. `http://gisr.tamu.edu/vision-mission`.

Department of Commerce (DOC); National Oceanic and Atmospheric Administration (NOAA), National Ocean Service (NOS), S. P. S. (1998, June). Galveston Bay, TX (G260) bathymetric digital elevation model (30 meter resolution) derived from source hydrographic survey soundings collected by NOAA. `estuarinebathymetry.noaa.gov/bathy_htmls/G260.html`.

Dinehart, R. L. and J. R. Burau (2005). Repeated surveys by acoustic Doppler current profiler for flow and sediment dynamics in a tidal river. *Journal of Hydrology 314*(1-4), 1–21.

Espinasse, B., M. Zhou, Y. W. Zhu, E. L. Hazen, A. S. Friedlaender, D. P. Nowacek, D. Z. Chu, and F. Carlotti (2012). Austral fall-winter transition of mesozooplankton assemblages and krill aggregations in an embayment west of the Antarctic Peninsula. *Marine Ecology Progress Series 452*, 63–80.

Filizola, N. and J. L. Guyot (2004). The use of Doppler technology for suspended sediment discharge determination in the River Amazon. *Hydrological Sciences Journal-Journal Des Sciences Hydrologiques 49*(1), 143–153.

Foreman, M. G. G.; Freeland, H. J. (1991). A comparison of techniques for tide removal from ship-mounted acoustic Doppler measurements along the southwest coast of Vancouver Island. *Journal of Geophysical Research-Oceans 96*(C9).

Fringer, O. B., M. Gerritsen, and R. L. Street (2006). An unstructured-grid, finite-volume, nonhydrostatic, parallel coastal ocean simulator. *Ocean Modelling 14*(3-4), 139–173. Fringer, O. B. Gerritsen, M. Street, R. L.

Geyer, W. R., J. H. Trowbridge, and M. M. Bowen (2000). The dynamics of a partially mixed estuary. *Journal of Physical Oceanography 30*(8), 2035–2048.

GoMRI (2013). About GoMRI. `http://gulfresearchinitiative.org/about-gomri/`.

Griffin, Felicia; Ashley, L. (2009). Mid-Bay Island. `http://betterbay.org/marshes_midbay.html`.

Henderson, F. (1969). *Open Channel Flow* (3rd ed.)., Chapter 1, pp. 2–3. The Macmillan Company.

Klinck, J. M., E. E. Hofmann, E. N. Powell, and M. M. Dekshenieks (2002). Impact of channelization on oyster production: a hydrodynamic-oyster population model for Galveston Bay, Texas. *Environmental Modeling & Assessment 7*(4), 273–289.

Lerczak, J. A., W. R. Geyer, and D. K. Ralston (2009). The temporal response of the length of a partially stratified estuary to changes in river flow and tidal amplitude. *Journal of Physical Oceanography 39*(4), 915–933.

MacCready, P. and W. R. Geyer (2010). *Advances in Estuarine Physics*, Volume 2 of *Annual Review of Marine Science*, pp. 35–58.

MacDonald, D. G. and W. R. Geyer (2004). Turbulent energy production and entrainment at a highly stratified estuarine front. *Journal of Geophysical Research-Oceans 109*(C5).

Marmorino, G. O. and C. L. Trump (1996). High-resolution measurements made across a tidal intrusion front. *Journal of Geophysical Research-Oceans 101*(C11), 25661–25674.

NOAA (2013a, November). Galveston Bay Operational Forecast System. `http://tidesandcurrents.noaa.gov/ofs/gbofs/gbofs.html`.

NOAA (2013b). National Data Buoy Center. `http://www.ndbc.noaa.gov`.

NOAA (2013c, October). Tides & Currents: Tidal Current Predictions for 2013. `http://tidesandcurrents.noaa.gov/currents13/tab2ac7.html#90`.

NOAA/NOS/CO-OPS (2013, November). NOAA/CO-OPS ODIN - NOAA Tides & Currents. http://tidesandcurrents.noaa.gov/map/.

O'Donnell, J., G. O. Marmorino, and C. L. Trump (1998). Convergence and downwelling at a river plume front. *Journal of Physical Oceanography 28*(7), 1481–1495.

Ojo, T. O., J. S. Bonner, and C. Page (2006). Studies on turbulent diffusion processes and evaluation of diffusivity values from hydrodynamic observations in Corpus Christi Bay. *Continental Shelf Research 26*(20), 2629–2644.

Old, C. P. and R. Vennell (2001). Acoustic Doppler current profiler measurements of the velocity field of an ebb tidal jet. *Journal of Geophysical Research-Oceans 106*(C4), 7037–7049.

Phillips, J. D., M. C. Slattery, and Z. A. Musselman (2004). Dam-to-delta sediment inputs and storage in the lower Trinity river, Texas. *Geomorphology 62*(1-2), 17–34.

Pinkel, R. (1979). Observations of strongly non-linear internal motion in the open sea using a range-gated Doppler sonar. *Journal of Physical Oceanography 9*(4), 675–686.

Port of Houston Authority (2012). Port of Houston Authority: Trade Statistics. http://www.portofhouston.com/business-development/trade-development-and-marketing/trade-statistics/.

Ralston, D. K., W. R. Geyer, and J. A. Lerczak (2008). Subtidal salinity and velocity in the Hudson River estuary: Observations and modeling. *Journal of Physical Oceanography 38*(4), 753–770.

Reed, R. E., H. B. Glasgow, J. M. Burkholder, and C. Brownie (2004). Seasonal physical-chemical structure and acoustic Doppler current profiler flow patterns over multiple years in a shallow, stratified estuary, with implications for lateral variability. *Estuarine Coastal and Shelf Science 60*(4), 549–566.

Sahl, L. E., W. J. Merrell, and D. C. Biggs (1993). The influence of advection on the spatial variability of nutrient concentrations on the Texas Louisiana Continental-Shelf. *Continental Shelf Research 13*(2-3), 233–251.

Schmalz, R. (2000, March). High-resolution Houston Ship Channel ADCP and CTD survey: Model-data intercomparisons. Technical report, NOAA.

Scully, M. E. and W. R. Geyer (2012). The role of advection, straining, and mixing on the tidal variability of estuarine stratification. *Journal of Physical Oceanography 42*(5), 855–868.

Sibley, M. M. (2013). Houston Ship Channel. https://www.tshaonline.org/handbook/online/articles/rhh11.

Sontek (2012, July). *RiverSurveyor S5/M9 System Manual Firmware Version 3.00*. 9940 Summers Ridge Road, San Diego, CA 92121-3091 USA: YSI.

Sontek/YSI (2012a). CastAway - CTD. `www.sontek.com/castaway`.

Sontek/YSI (2012b). RiverSurveyor S5 and M9. `http://www.sontek.com/riversurveyor-s5-m9.php`.

Szupiany, R. N., M. L. Amsler, J. L. Best, and D. R. Parsons (2007). Comparison of fixed- and moving-vessel flow measurements with an aDp in a large river. *Journal of Hydraulic Engineering-Asce 133*(12), 1299–1309.

Trowbridge, J. H., W. R. Geyer, M. M. Bowen, and A. J. Williams (1999). Near-bottom turbulence measurements in a partially mixed estuary: Turbulent energy balance, velocity structure, and along-channel momentum balance. *Journal of Physical Oceanography 29*(12), 3056–3072.

USGS (2013, November). Usgs current water data for texas.

Velasco, David; Sloat, J. (2012, December). Velocity mapping, navigation and depth sounding with the SonTek HydroSurveyor.

Warnken, K. W., G. A. Gill, L. L. Griffin, and P. H. Santschi (2001). Sediment-water exchange of Mn, Fe, Ni and Zn in Galveston Bay, Texas. *Marine Chemistry 73*(3-4), 215–231.

Warnken, K. W., G. A. Gill, P. H. Santschi, and L. L. Griffin (2000). Benthic exchange of nutrients in Galveston Bay, Texas. *Estuaries 23*(5), 647–661.

Warnken, K. W. and P. H. Santschi (2009). Delivery of trace metals (Al, Fe, Mn, V, Co, Ni, Cu, Cd, Ag, Pb) from the Trinity River watershed towards the ocean. *Estuaries and Coasts 32*(1), 158–172.

Wermund, E.G.; Morton, R. A. P. G. (1989). Galveston Bay: Issues, resources, status and management. Technical report, NOAA Estuarine Programs Office, Washington, DC.

WHOI (2011, September). WHOI-led study sharpens picture of how much oil and gas flowed in Deepwater Horizon Spill. `http://www.whoi.edu/page.do?pid=7545&tid=3622&cid=112889`.

Yeager, K. M., P. H. Santschi, H. S. Rifai, M. P. Suarez, R. Brinkmeyer, C. C. Hung, K. J. Schindler, M. J. Andres, and E. A. Weaver (2007). Dioxin chronology and fluxes in sediments of the Houston Ship Channel, Texas: Influences of non-steady-state sediment transport and total organic carbon. *Environmental Science & Technology 41*(15), 5291–5298.

Zhou, M., W. Nordhausen, and M. Huntley (1994). ADCP measurements of the distribution and abundance of euphausiids near the Antarctic Peninsula in winter. *Deep-Sea Research Part I-Oceanographic Research Papers 41*(9), 1425–1445.